

POLYMORPHISM IN SOLID 1,1,1-TRICHLOROETHANE
AND SOLID 2,2-DICHLOROPROPANE

POLYMORPHISM IN SOLID 1,1,1-TRICHLOROETHANE
AND SOLID 2,2-DICHLOROPROPANE

BY

MARGARET SAKON, B.A.

A Thesis

Submitted to the School of Graduate Studies
in Partial Fulfillment of the Requirements
for the Degree
Master of Science

McMaster University

August, 1976

MASTER OF SCIENCE (1976)
(Chemistry)

McMASTER UNIVERSITY
Hamilton, Ontario

TITLE: Polymorphism in Solid 1,1,1-trichloroethane
and Solid 2,2-dichloropropane

AUTHOR: Margaret Sakon, B.A. (The University of
Lethbridge)

SUPERVISOR: Professor J. A. Morrison

NUMBER OF PAGES: viii,55

ABSTRACT

The methylchloromethane (MCM) compounds $((\text{CH}_3)_n \text{C Cl}_{(n-4)})$ with $0 < n < 4$ exist in several different solid phases (or polymorphs). The high temperature solid phases of the compounds come under Timmermans' classification of "plastic" crystals. The discovery of a second plastic polymorph of CCl_4 by Post (1959) led to extensive X-ray and differential scanning calorimetric (DSC) studies of the entire group of MCM compounds. The present research deals specifically with 1,1,1-trichloroethane ($n=1$) and 2,2-dichloropropane ($n=2$). Optical birefringence of the different solid phases has been measured with the object of obtaining information about their structures, their stabilities and the sequences of their transformations from one phase to another. The results of the investigation lead to conclusions that differ somewhat from those derived from X-ray and DSC studies. For example, the plastic crystal phases of 1,1,1-trichloroethane are not both cubic, as earlier X-ray measurements indicated, and their stabilities seem to depend upon the purities of the specimens. The sequence of phase transitions also differs from that found in DSC studies.

2,2-dichloropropane has three solid phases and only one is cubic. The cubic phase is unusually stable; this may be attributable to a stabilizing influence of the surface (glass) of the sample cell. The optical birefringence results give a different view of the transitions than that deduced from existing meagre thermal data.

The information gleaned from the optical birefringence measurements has subsequently led to an extensive investigation of the thermal properties of 1,1,1-trichloroethane with a high precision adiabatic calorimeter. It has confirmed the general description of the interrelation between the different phases given here as well as the strategic role played by impurities.

TABLE OF CONTENTS

| CHAPTER | | <u>Page</u> |
|---------|--|-------------|
| 1 | INTRODUCTION | 1 |
| | 1.1 Polymorphism and Plastic Crystals | 1 |
| | 1.2 The Methylchloromethane Compounds | 3 |
| 2 | BIREFRINGENCE | 10 |
| | 2.1 Background for Experimental Measurements | 10 |
| | 2.2 Calculation of Birefringence from Theory | 15 |
| 3 | EXPERIMENTAL TECHNIQUES | 18 |
| | 3.1 Method A | 18 |
| | A Theoretical Aspects of Measurement | 18 |
| | B The Optical System | 21 |
| | C The Optical Cell | 23 |
| | D Method of Measurement | 23 |
| | 3.2 Method B | 24 |
| | 3.3 Thermal Analysis | 25 |
| | 3.4 Materials | 27 |
| 4 | RESULTS | 28 |
| | 4.1 Thermal Analysis | 28 |
| | 4.2 Birefringence | 35 |
| 5 | DISCUSSION | 47 |
| 6 | CONCLUSIONS | 52 |
| | REFERENCES | 54 |

LIST OF TABLES

| TABLE | | <u>Page</u> |
|-------|--|-------------|
| 1.1 | X-ray Data for Methylchloromethane (MCM) Compounds | 4 |
| 1.2 | Transition Temperatures for Different Phases of MCM Compounds | 5 |
| 1.3 | Heats and Entropies of Transitions between Different Phases of MCM Compounds | 6 |
| 4.1 | Temperatures of Phase Changes from the Thermal Analyses of MCF and DCP | 36 |
| 4.2 | Birefringence of the Solid Phases of MCF and DCP | 39 |
| 4.3 | Temperatures of Phase Changes from the Birefringence Study of MCF and DCP | 40 |
| 5.1 | Summary of Calorimetric Measurements on MCF | 49 |

LIST OF FIGURES

| FIGURE | | <u>Page</u> |
|--------|---|-------------|
| 2.1 | Indicatrices for a uniaxial crystal | 12 |
| 2.2 | Indicatrix for a biaxial crystal | 12 |
| 2.3 | Random wave normal and extraordinary and ordinary rays | 14 |
| 2.4a | Wave normal perpendicular to optic axis | 14 |
| 2.4b | Wave normal parallel to optic axis | 14 |
| 2.5 | Types of intersection between the faces of a crystal and its indicatrix | 16 |
| 3.1 | Parameters used in analysis of birefringence measurements | 19 |
| 3.2 | Details of optical system | 22 |
| 3.3 | Apparatus for thermal analysis | 26 |
| 4.1a | Portion of a cooling curve for MCF(I) (thermal analysis) | 29 |
| 4.1b | Portion of a heating curve for MCF(I) (thermal analysis) | 30 |
| 4.2a | Portion of a cooling curve for DCP (thermal analysis) | 31 |
| 4.2b | Portion of a heating curve for DCP (thermal analysis) | 32 |
| 4.3 | Plot of $ K_{eff} $ versus temperature for MCF | 33 |
| 4.4 | Plot of $ K_{eff} $ versus temperature for DCP | 34 |
| 4.5 | Phase changes in MCF(I) deduced from thermal analyses | 37 |

| FIGURE | | <u>Page</u> |
|--------|--|-------------|
| 4.6 | Phase changes in DCP deduced from thermal analyses | 37 |
| 4.7a | Plot of temperature versus time for DCP (birefringence measurements) | 42 |
| b | | 43 |
| c | | 44 |
| d | | 45 |
| 4.8 | Phase transitions in MCF and DCP deduced from birefringence studies. | 46 |

CHAPTER 1
INTRODUCTION

1.1 Polymorphism and Plastic Crystals

Polymorphism in crystals simply means that different crystal structures are formed by the same substance. The structures may be stable or metastable but will usually be characterized by well-defined physical properties such as melting points, heat capacities, etc.

The labelling of polymorphs is an arbitrary procedure but it is most convenient to use numbers or letters sequentially from the highest temperature down. The subsequent discovery of additional phases, in overlapping temperature regions, can be accommodated by using the designations Ia, Ib, --- or α , α' --- etc.

For molecular crystals, one would expect the crystal symmetry of the polymorphs to decrease with decreasing temperature. This can be rationalized because the principal cause of polymorphic change must be orientational ordering or disordering of the molecules on their lattice sites. At low temperatures, the thermal energy is insufficient to surmount the potential barriers that restrict or hinder rotation of the molecules so that the molecular orientations become subject

to asymmetric intermolecular forces.

A simple view of molecular solids might be to consider the existence of a temperature-dependent equilibrium between two kinds of molecules - "rotational" and "librational". This model has been presented by Chihara and Koga (1971). They proposed that, at the transition temperature, there would be an abrupt displacement of the equilibrium. At the rotational transition point, the fraction of rotating molecules (i.e. the fraction of molecules with sufficient energy to overcome potential barriers to rotation) in the lower temperature phase is of the magnitude of $1/60$ of the total number of molecules and that this fraction is sufficient to "trigger" the transition. The transition would proceed with the motions of the molecules influencing one another cooperatively. The transition would be completed when the fraction of rotating molecules became $1/3$ of the total.

The highest temperature polymorphs of some molecular crystals are classified by the term "plastic". This term was first used by Timmermans (see, for example, Timmermans (1961) for a general discussion) to describe molecular crystals with low entropies of fusion (less than 5 e.u.), high melting points and low enthalpies of fusion. As the name implies, plastic crystals deform rather easily. To achieve a given strain rate, the stress that needs to be applied to a plastic crystal is only a few percent of that needed for a non-plastic crystal of comparable chemical constitution. In general, plastic crystal

phases are only formed by systems of globular-shaped molecules. When globular and non-globular isomers are compared, e.g. neopentane with n-pentane, the liquid temperature range of the latter roughly corresponds to the plastic crystal plus liquid ranges of the former (Timmermans, 1961).

The structure of plastic crystals is always one of high symmetry (usually cubic). A cubic structure implies that the molecules can reorient without serious hindrance. Thus, in many plastic crystals, as the temperature is lowered below the freezing point, the dielectric constant either drops slightly or may even continue to rise until it drops sharply when a lower transition point is reached. In non-plastic crystals, the dielectric constant drops sharply at the freezing point.

1.2 The Methylchloromethane Compounds

The methylchloromethane (MCM) compounds (i.e. the compounds with the structural formula $(\text{CH}_3)_n \text{C Cl}_{(4-n)}$, where $0 < n < 4$), which are the subject of this thesis, come under Timmermans' classification of globular molecules. Through much experimental investigation, it was established that all of them form at least one plastic crystal phase in the solid state. The most extensive investigations have been carried out at Adelphi University by R. Rudman and colleagues who have used the techniques of single crystal X-ray diffraction and differential scanning calorimetry (Rudman and Post, 1966 and 1968; Rudman, 1970; Silver and Rudman, 1970 and 1972). Tables 1.1, 1.2 and 1.3 summarize the structural and thermal data

TABLE 1.1 *X-ray Data for Methylchloromethane (MCM) Compounds

| Carbon tetrachloride CCl ₄ | | Methyl chloroform CH ₃ C Cl ₃ | | 2,2-dichloropropane (CH ₃) ₂ C Cl ₂ | | t-butyl chloride (CH ₃) ₃ C Cl | | Neopentane (CH ₃) ₄ C | |
|--|--------------|--|--------------|--|--------------|--|------------|---|-----------|
| Liquid | Phase Ia | Phase Ib | Phase Ia | Phase Ib | Phase Ia | Phase Ib | Liquid | Phase I | Liquid |
| | f.c.c. | Rhombo- hedral | f.c.c. | Cubic | f.c.c. | Rhombo- hedral | f.c.c. | f.c.c. | f.c.c. |
| a=8.34 | a=8.39 | a=14.42 | a=8.39 | a=14.61 | a=8.45 | a=14.68 | a=8.62 | a=8.82 | a=8.82 |
| α=90.0° | | α=90.0° | | | | α=90.0° | | | |
| Phase II | Phase II | Phase II | Phase II | Phase II | Phase II | Phase II | Phase II | Phase II | Phase II |
| Monoclinic | Orthorhombic | Orthorhombic | Orthorhombic | Orthorhombic | Orthorhombic | Orthorhombic | Tetragonal | Hexagonal | Hexagonal |
| a=20.3 | a=7.92 | a=7.92 | a=7.92 | a=9.67 | a=9.67 | b=6.09 | a=7.08 | a=14.3 | a=14.3 |
| b=11.6 | b=11.2 | b=11.2 | b=11.2 | c=9.40 | c=9.40 | b=6.09 | c=6.14 | c=8.84 | c=8.84 |
| c=19.9 | c=5.78 | c=5.78 | c=5.78 | | | | | | |

Crystal system

Unit cell Dimensions (Å°)

* Data taken from Rudman and Post (1968) and Rudman (1970)

TABLE 1.2 *Transition Temperatures for Different Phases of MCM Compounds

| CCl_4 | $\text{CH}_3 \text{ C Cl}_3$ | $(\text{CH}_3)_2 \text{ C Cl}_2$ | $(\text{CH}_3)_3 \text{ C Cl}$ | $(\text{CH}_3)_4 \text{ C}$ |
|--|---|---|--|--|
| <p>Liquid</p> <p>↙ 245.2 ↘</p> <p>↙ 247.8 ↘</p> <p>↙ 244.8 ↘</p> <p>↙ 234.0 ↘</p> <p>↙ 217.3 ↘</p> <p>↙ 226.6 ↘</p> <p>Phase Ia</p> <p>↔ 234.0 ↔</p> <p>Phase Ib</p> <p>↔ 217.3 ↔</p> <p>↔ 226.6 ↔</p> <p>Phase II</p> | <p>Liquid</p> <p>↙ 227 ↘</p> <p>↙ 231.9 ↘</p> <p>↙ 214.3 ↘</p> <p>↙ 178 ↘</p> <p>↙ 220.5 ↘</p> <p>Phase Ia</p> <p>↔ 214.3 ↔</p> <p>Phase Ib</p> <p>↔ 178 ↔</p> <p>↔ 220.5 ↔</p> <p>Phase II</p> | <p>Liquid</p> <p>↙ ? ↘</p> <p>↙ 226.7 ↘</p> <p>↙ 184.8 ↘</p> <p>↙ 187.0 ↘</p> <p>Phase Ia</p> <p>↔ 184.8 ↔</p> <p>Phase Ib</p> <p>↔ 187.0 ↔</p> <p>Phase II</p> | <p>Liquid</p> <p>↙ 245.2 ↘</p> <p>↙ 250.3 ↘</p> <p>↙ 209.8 ↘</p> <p>↙ 178.5 ↘</p> <p>↙ 181.0 ↘</p> <p>Phase I</p> <p>↔ 245.2 ↔</p> <p>↔ 250.3 ↔</p> <p>↔ 209.8 ↔</p> <p>↔ 178.5 ↔</p> <p>↔ 181.0 ↔</p> <p>Phase II</p> <p>↔ 181.0 ↔</p> <p>Phase III</p> | <p>Liquid</p> <p>↙ 255 ↘</p> <p>↙ 253.6 ↘</p> <p>↙ 134.4 ↘</p> <p>↙ 139.0 ↘</p> <p>Phase I</p> <p>↔ 255 ↔</p> <p>↔ 253.6 ↔</p> <p>↔ 134.4 ↔</p> <p>↔ 139.0 ↔</p> <p>Phase II</p> |

Transition Temperatures (°K)

*Data taken from Silver and Rudman (1970)

TABLE 1.3 *Heats and Entropies of Transitions between Different Phases of MCM Compounds

| CCl_4 | $\text{CH}_3 \text{ C Cl}_3$ | $(\text{CH}_3)_2 \text{ C Cl}_2$ | $(\text{CH}_3)_3 \text{ C Cl}$ | $(\text{CH}_3)_4 \text{ C}$ |
|---|---|--|---|--|
| <p>Liquid</p> <p>Phase Ia $\xrightarrow{-164}$ Phase Ib</p> <p>Phase Ia $\xrightarrow{-0.70}$ Phase II</p> <p>Liquid $\xrightarrow{596}$ Phase Ia</p> <p>Liquid $\xrightarrow{419}$ Phase Ib</p> <p>Liquid $\xrightarrow{-407}$ Phase Ia</p> <p>Liquid $\xrightarrow{-1.66}$ Phase Ib</p> <p>Phase Ia $\xrightarrow{2.41}$ Phase Ib</p> <p>Phase Ia $\xrightarrow{1.71}$ Phase Ib</p> <p>Phase Ia $\xrightarrow{-1063}$ Phase II</p> <p>Phase Ia $\xrightarrow{-4.89}$ Phase II</p> <p>Phase Ia $\xrightarrow{1070}$ Phase II</p> <p>Phase Ia $\xrightarrow{4.72}$ Phase II</p> | <p>Liquid</p> <p>Phase Ia $\xrightarrow{-162}$ Phase Ib</p> <p>Phase Ia $\xrightarrow{-0.76}$ Phase II</p> <p>Liquid $\xrightarrow{451}$ Phase Ia</p> <p>Liquid $\xrightarrow{217}$ Phase Ib</p> <p>Liquid $\xrightarrow{-226}$ Phase Ia</p> <p>Liquid $\xrightarrow{-0.99}$ Phase Ib</p> <p>Phase Ia $\xrightarrow{1.87}$ Phase Ib</p> <p>Phase Ia $\xrightarrow{0.93}$ Phase Ib</p> <p>Phase Ia $\xrightarrow{-1433}$ Phase II</p> <p>Phase Ia $\xrightarrow{-8.09}$ Phase II</p> <p>Phase Ia $\xrightarrow{1227}$ Phase II</p> <p>Phase Ia $\xrightarrow{5.56}$ Phase II</p> | <p>Liquid</p> <p>Phase Ia $\xrightarrow{537}$ Phase Ib</p> <p>Phase Ia $\xrightarrow{-1373}$ Phase II</p> <p>Liquid $\xrightarrow{-544}$ Phase Ia</p> <p>Liquid $\xrightarrow{-2.40}$ Phase Ib</p> <p>Phase Ia $\xrightarrow{1415}$ Phase II</p> <p>Phase Ia $\xrightarrow{7.57}$ Phase II</p> | <p>Liquid</p> <p>Phase I $\xrightarrow{410}$ Phase II</p> <p>Phase I $\xrightarrow{-1298}$ Phase II</p> <p>Liquid $\xrightarrow{-414}$ Phase I</p> <p>Liquid $\xrightarrow{-1.69}$ Phase II</p> <p>Phase I $\xrightarrow{1281}$ Phase II</p> <p>Phase I $\xrightarrow{-6.19}$ Phase II</p> <p>Phase I $\xrightarrow{-401}$ Phase-III</p> <p>Phase I $\xrightarrow{-2.25}$ Phase-III</p> | <p>Liquid</p> <p>Phase I $\xrightarrow{774}$ Phase II</p> <p>Phase I $\xrightarrow{-623}$ Phase II</p> <p>Liquid $\xrightarrow{-724}$ Phase I</p> <p>Liquid $\xrightarrow{-2.84}$ Phase II</p> <p>Phase I $\xrightarrow{612}$ Phase II</p> <p>Phase I $\xrightarrow{-4.64}$ Phase II</p> |

1. ΔH_t (cal/mol)

2. ΔS_t (cal/mol deg)

* Data taken from Silver and Rudman (1970)

derived by them. Although the results are extensive, some general and some specific questions persist regarding the structures and stabilities of some of the phases as well as the sequences of the transitions.

The questions arise mainly because of the difficulty in controlling the temperature of the X-ray sample and in varying the temperature smoothly. This meant that it was difficult to maintain the X-ray specimens in a particular state for a long time. In DSC experiments, the problem of obtaining thermal equilibrium arises, especially in the region of phase transitions, where considerable molecular reorientation is taking place and the heat capacities take on large values. This makes the transition temperatures imprecise and is indicated by the different transition temperatures obtained on heating and cooling the sample through the transitions. In both methods, the specimen studied was very small so that purity levels were uncertain. In the birefringence experiments to be described in this thesis, the apparatus permitted close observation of the various phases for days at constant temperature (within one degree).

In the case of CCl_4 , which has been previously reported to melt at $250^\circ K$ and to have a solid transition at $225^\circ K$ (Hicks, Hooley and Stephenson, 1944), the discovery of a third phase existing in the temperature range of phase I (Post, 1959), initiated the research of the MCM compounds by Rudman and colleagues. The new phase which formed on freezing CCl_4 was called phase Ia and was found to be face-centred cubic.

The phase obtained by previous researchers was called phase Ib and was thought to be weakly birefringent. This birefringence was verified with a highly sensitive and accurate technique (Koga and Morrison, 1975). It was also found that phase Ia and Ib can co-exist under certain conditions and that the phase Ia-to-phase Ib transition was reversible. This reversibility is not observed in calorimetric measurements (Morrison and Richards, 1976) which suggests that the nature of the sample container may be important. (The birefringence cell was made of glass whereas the calorimetric vessel was made of copper.)

The question then arose as to whether the other MCM compounds undergo similar phase transitions. Silver and Rudman (1970) found no evidence of a phase Ib in t-butyl chloride nor in neopentane. However, they did find a phase Ia and phase Ib in both methyl chloroform (1,1,1-trichloroethane which will be abbreviated to MCF) and 2,2-dichloropropane (DCP). They determined that the phase Ia's in both compounds had face-centred cubic structures while phase Ib was primitive cubic in MCF and rhombohedral in DCP.

Birefringence measurements can provide a valuable check on such structural deductions. At any particular temperature, the crystals may be cubic and therefore non-birefringent or of slightly lower than cubic symmetry and thus weakly birefringent ($|n_e - n_o| \sim 10^{-3}$) or of very low symmetry giving strongly birefringent crystals ($|n_e - n_o| > 10^{-3}$).

An apparatus for crude thermal analysis was devised in order to provide a guide for the birefringence

ments by giving the temperature regions for the existence of the different phases.

Thus, this research was started with the purpose of providing information about particular crystal polymorphs and the transitions between them. MCF and DCP were investigated because there seemed to be significant uncertainties in the characterization of their phases. The birefringence measurements on MCF subsequently led to an extensive calorimetric study of that substance (Morrison, Richards and Sakon, 1976).

CHAPTER 2

BIREFRINGENCE

2.1 Background for Experimental Measurements

Birefringence or double refraction refers to the existence of more than one refractive index in a crystal. Monochromatic light passing into a birefringent crystal splits into two plane polarized waves vibrating in different directions and often following two different ray paths. The ordinary ray obeys Snell's Law while the extraordinary ray does not. Snell's Law is expressed as

$$n_i \sin i = \omega \sin r_o, \quad (2.1)$$

where n_i is the refractive index of the medium through which the incident light has travelled; i is the angle of the incident light and ω is the refractive index of the medium along the ray path defined by the angle of the refracted ordinary ray, r_o . A description of the optics involved in birefringence measurements can be found in Bloss (1961). It is briefly summarized in this section and the figures are taken from or adapted from figures in the reference.

The concept of the optical indicatrix was devised to illustrate the relationship between the refractive index of a material and the vibration direction of the light waves

travelling in the material. The indicatrix is a surface connecting vectors radiating from a common point in the material and proportional to the refractive index for light vibrating parallel to the corresponding vector direction. In isotropic media (including cubic solids), the refractive index is the same in any vibration direction and so the indicatrix is a sphere.

In an anisotropic medium, the indicatrix is an ellipsoid. There may be either two principal axes (and therefore two principal refractive indices) or three principal axes (with three principal refractive indices) perpendicular to each other. In the former case, the indicatrix is an ellipsoid. The indicatrix can resemble either of the two geometrics shown in figure 2.1. The central section, perpendicular to the principal symmetry axis, and only this section, is a circle (with radius ω). The principal symmetry axis is called the optic axis and the crystals are said to be uniaxial. ϵ and ω are called the extraordinary and ordinary refractive indices, respectively, but are often represented by n_e and n_o .

When there are three principal axes, the indicatrix is a triaxial ellipsoid as shown in figure 2.2. X, Y and Z represent the principal axes and α , β and γ the corresponding principal refractive indices. γ and α are the maximum and minimum refractive indices respectively and β an intermediate value. Any other vector drawn from the center to the surface of the indicatrix is some value between γ and α (e.g. γ' , α' and β). There are two circular sections, both of which contain the principal axis of the indicatrix that is intermediate in

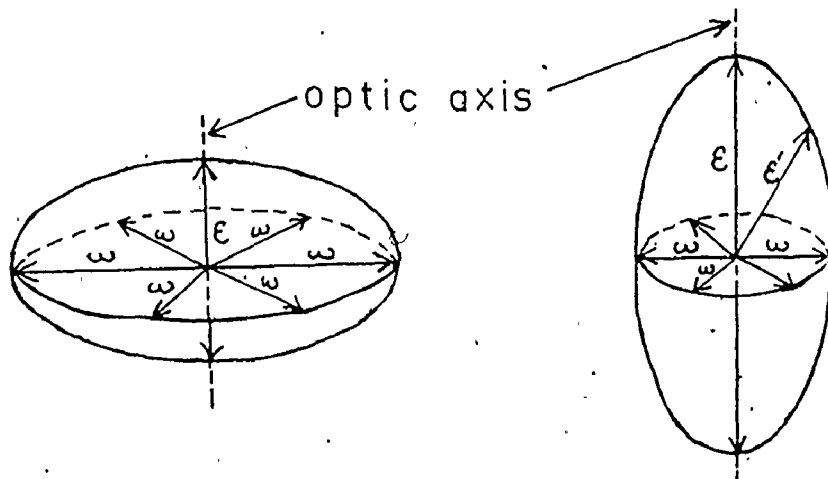


Figure 2.1 Indicatrices for a uniaxial crystal

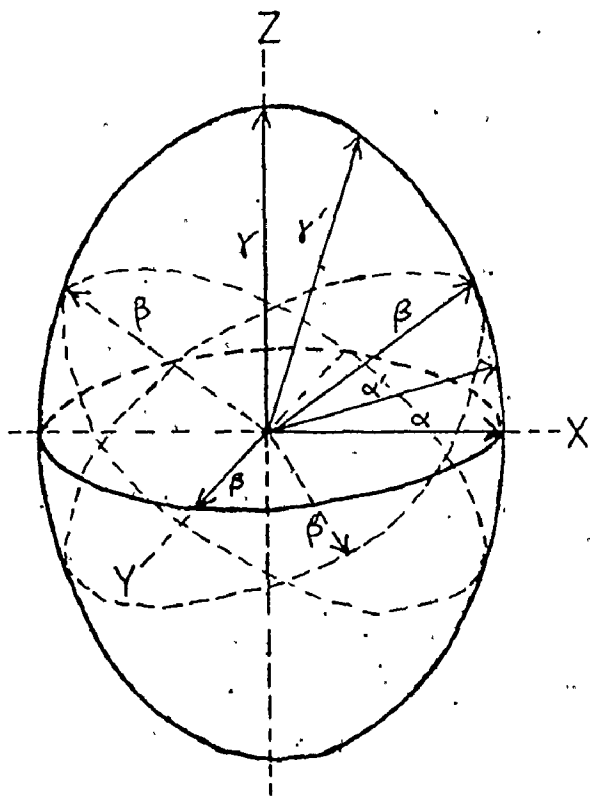


Figure 2.2 Indicatrix for a biaxial crystal

length between the other two. Their radius is thus equal to the intermediate principal refractive index, β . Thus, there are two optic axes perpendicular to the two circular sections and the crystals are described as being biaxial.

In a uniaxial crystal, any central section in its indicatrix will always have one principal axis equal to ω (see figure 2.3). The other principal axis will be intermediate in length between ω and ϵ . Two waves propagating outwards from a point source (say in the center of the indicatrix) can travel in any direction. One of them always has the same refractive index ω , and therefore the same velocity, regardless of direction; the other has a refractive index that varies from ω to ϵ according to the direction of the wave normal. The direction of the wave normal lies in the same plane as the ray path and vibration direction and is perpendicular to the vibration direction. If the vibration direction is perpendicular to the ray path (which is always the case for the ordinary ray), the wave normal corresponds to the ray path.

Figure 2.3 shows a random wave normal with the ordinary and extraordinary waves vibrating in planes perpendicular to the normal. The wave normal is OW and is the same as the ordinary ray. The vibration direction of the ordinary wave is parallel to ω . OR_E is the extraordinary ray and the vibration direction of the extraordinary wave is ϵ' .

In the simpler situations where the incident light is perpendicular or parallel to the optic axis, the paths of the two rays are the same and also coincide with the wave normal.

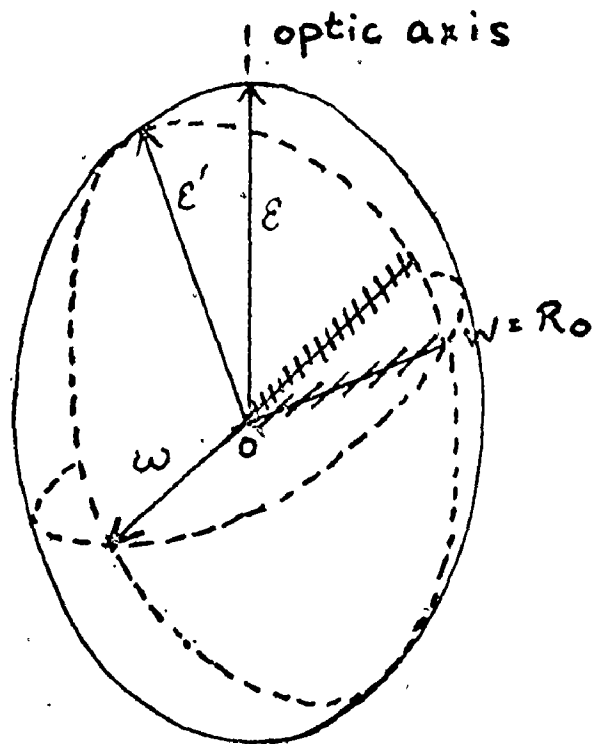


Figure 2.3 Random wave normal and extraordinary and ordinary rays

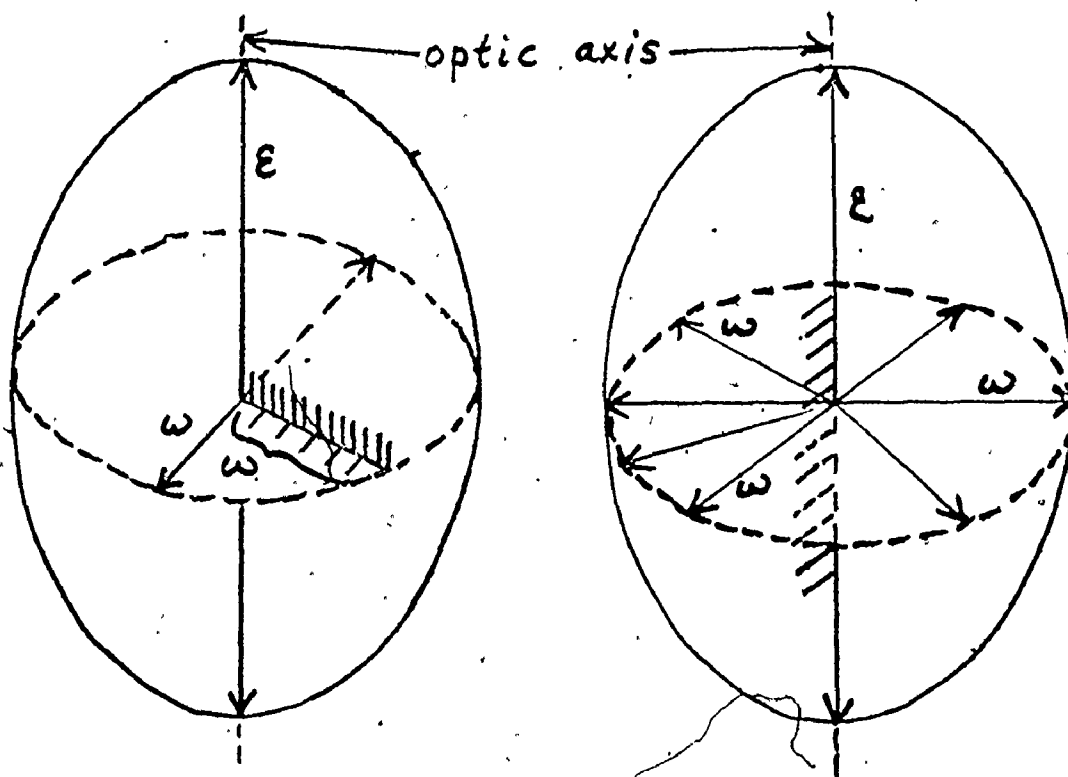


Figure 2.4a Wave normal perpendicular to optic axis

Figure 2.4b Wave normal parallel to axis

In figure 2.4a where the wave normal is perpendicular to the optic axis, the wave vibration direction of an ordinary ray is parallel to a vector corresponding to the refractive index ω , and the wave vibration direction for the extraordinary ray is parallel to the vector corresponding to the refractive index ϵ . In figure 2.4b, where the wave normal is parallel to the optic axis, the refractive index is ω (no double refraction). Plane polarized light parallel to the optic axis passes through the crystal unaltered in direction.

For normal incidence on a crystal surface, the directions of vibration of the two refracted rays can be visualized if the crystal's indicatrix is drawn with its center on the crystal face (figure 2.5). The intersection between the indicatrix and the crystal face is either an ellipse or a circle.

In the birefringence measurements only those crystals that were oriented such that the principal axes in the indicatrix were perpendicular to the incident light were considered.

2.2 Calculation of Birefringence from Theory

In an ideal situation where the crystal structure is known and is not too complicated, and where polarizabilities of the constituent ions or molecules are available, the birefringence of the crystal may be calculated. The principle of the calculation was developed many years ago by Ewald (see Born and Huang, 1954, for a discussion of it), and a method suitable for the modern computer was published by Cowley (1970).

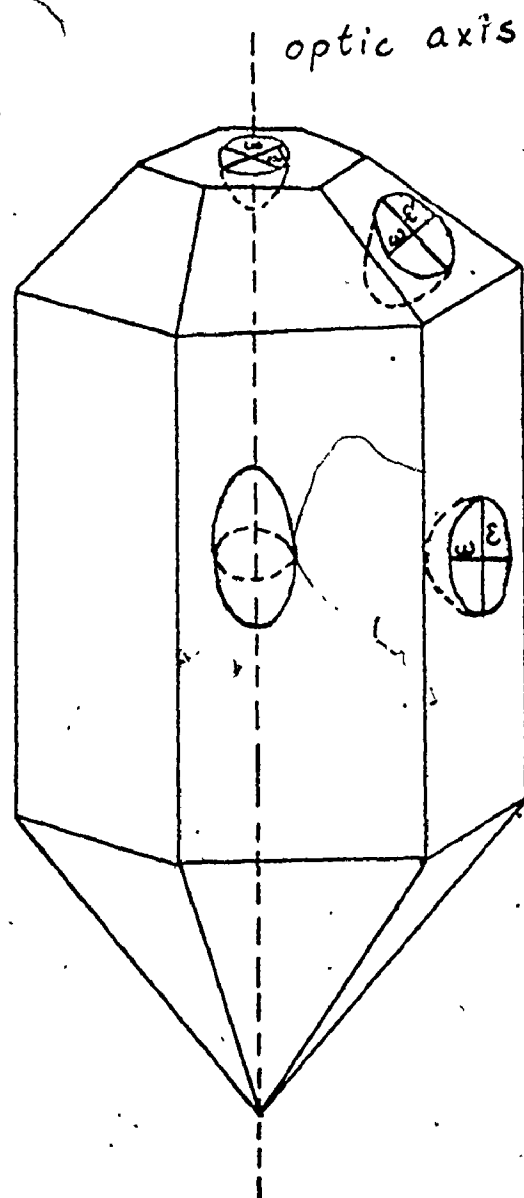


Figure 2.5 Types of intersection between the faces of a crystal and its indicatrix. The heavy radii of the ellipse (or circle) indicate the crystal's privileged directions for light entering by normal incidence on this face. (Taken from Bloss, 1961 p.82)

For MCF and DCP, the detailed structure of phase Ib is unknown and accurate values of the polarizability of the molecules are unavailable. Hence, a theoretical estimate of the birefringence cannot be made. For MCF the structure of phase II is known and the experimental value of $|n_e - n_o|$ is consistent with an order of magnitude calculation using Cowley's method (Morrison et al, 1976).

CHAPTER 3
EXPERIMENTAL TECHNIQUES

Two methods of estimating the birefringence of the crystal phases were employed. One technique (method A) was used to measure very small birefringences in order to verify the existence of cubic phases. (Slight ambiguity resulted because of small birefringences caused by strain and imperfections in the system.) This technique is capable of determining birefringences between 5×10^{-6} and 1×10^{-3} . Larger birefringences were estimated using an Interference Colour Chart (Bloss, 1961) (method B).

3.1 Method A

A. Theoretical Aspects of Measurement

In figure 3.1, which is taken from Ballik et al (1973), the plane which contains the given axes is normal to the incident beam. The axes n_1 and n_2 represent the crystal's principal indices. E_i represents the plane-polarized incident beam and E_t represents the beam transmitted through the analyzer.

For an isotropic ($n_1 = n_2$) medium and crossed polarizers in an ideal optical system, the beam is completely extinguished at the analyzer when the coupled polarizers are rotated. The reason for this is that the incident beam passes through the crystal in the same vibration direction of the wave as it does

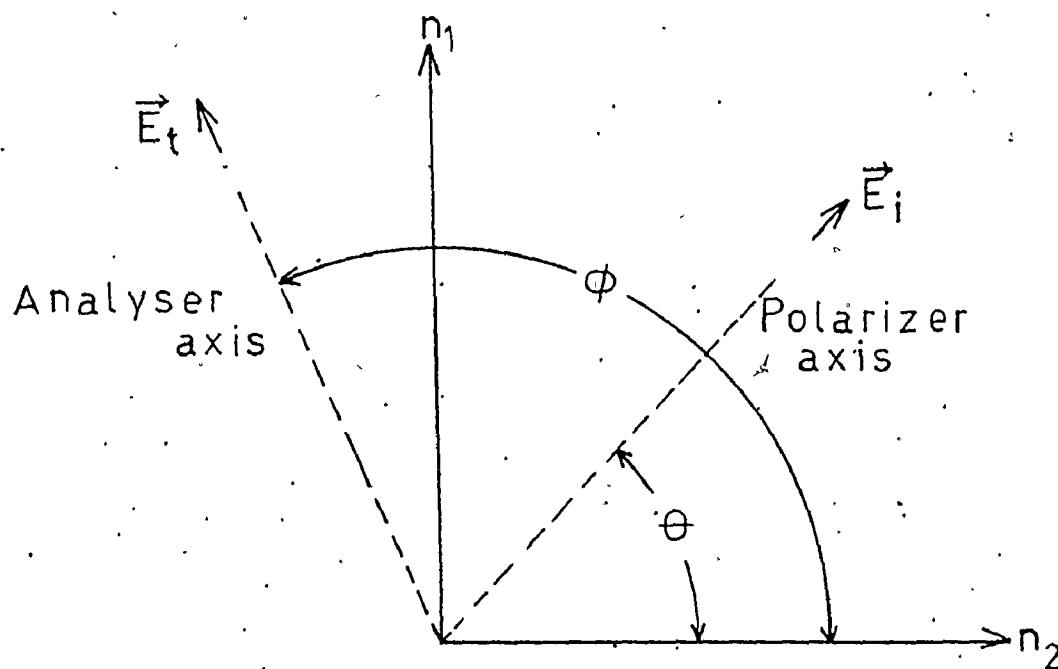


Figure 3.1 Parameters used in analysis of birefringence measurements

on entering (since the refractive index is the same in any vibration direction). For parallel polarizers, the analyzer transmits a beam of the same intensity as that transmitted by the polarizer.

In anisotropic media, the incident polarized beam passes unaltered in the vibration direction of the wave only if it corresponds to either of the principal axes, n_1 or n_2 . Thus under crossed polarizers, the beam is extinguished again. (In practice, a minimum intensity is obtained.) The angles at which minimum intensities occur give the directions of n_1 and n_2 .

Ideally, the maximum intensities occur at 45° , 135° , 225° and 315° from the angles of minimum intensity. The incident beam is split into a slow wave and a fast wave in the crystal and can be resolved into two vector components corresponding in direction to n_1 and n_2 . The waves emerging from the crystal have a phase difference, α . That is, the fast wave has travelled a distance α by the time the slow wave emerges from the crystal. α varies with the crystal thickness, the wavelength of the incident light and n_1 and n_2 . The intensity transmitted by the analyzer, I_t , is thus related to the angle and amplitude (and therefore intensity) of the incident light, the phase difference and the angle of the analyzer. For an incident beam normal to both axes n_1 and n_2 in a crystal of thickness, d ,

$$I_t = I_i (\sin^2 \theta \sin^2 \phi + \cos^2 \theta \cos^2 \phi + 2 \sin \theta \cos \theta \sin \phi \cos \phi \cos \alpha), \quad (3.1)$$

where $\alpha = (2\pi d/\lambda)(n_2 - n_1)$,

and λ is the mean wavelength of the filtered source.

A value for α and, therefore $|n_2 - n_1|$, can be obtained from the ratio of the transmitted light intensities for crossed and parallel polarizers (I_{\perp}/I_{\parallel}) set at the angles of maximum intensity. The equation is

$$I_{\perp}/I_{\parallel} = \tan^2 (\alpha/2) \quad (3.2)$$

The derivation of equation 3.2 is given in the paper by Ballik et al (1973) and will not be repeated here.

For any one value of I_{\perp}/I_{\parallel} , there are several possible values of α . In order to obtain a unique value of α and therefore of $|n_2 - n_1|$, measurements need to be made with two or more wavelengths of light. An example of the calculations is given in appendix A of the paper by Ballik et al (1973).

B. The Optical System

The optical system was the same as that used for measuring birefringence in the solid isotopic methanes (Ballik, Gannon and Morrison, 1973) and was set up according to figure 3.2 (taken from that reference). The light source was a tungsten filament lamp. The wavelength of the light is altered by using bandpass filters of wavelengths 4400 and 5600 Å. The light is then focused by the first lens into the center of the cell. The polarizer produces a linearly-polarized beam which passes through the cell and the second polarizer (analyzer). The analyzer is mechanically coupled to the polarizer such that their transmission axes are either parallel or perpendicular to each other and that the coupled polarizers can rotate

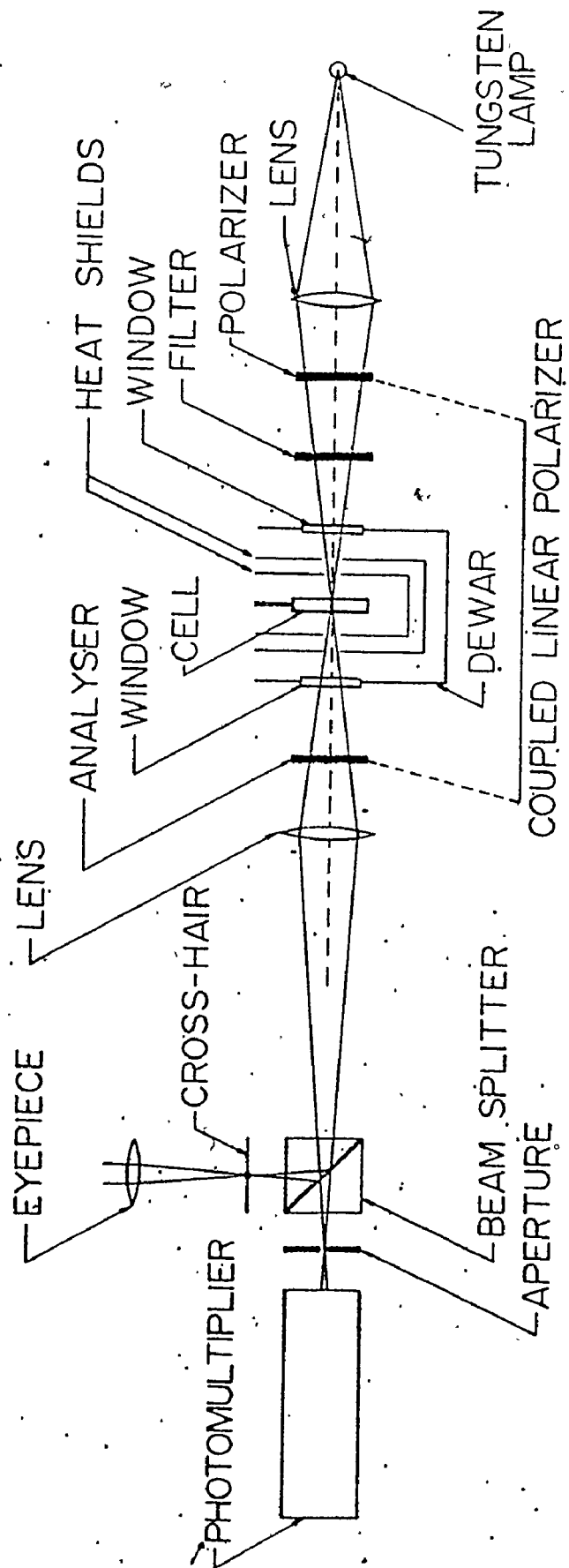


Figure 3.2 Details of the optical system

through 360° . The second lens focuses light from the center of the cell toward the beam splitter where two images are formed. One is formed at the cross-hair at an eyepiece and the other at the aperture where it passes through to the photomultiplier. The output of the photomultiplier was read from a Keithley multimeter (model 171). The crystal section that could be viewed was about 1.6 mm in diameter but the area seen by the photomultiplier was no more than 0.035 mm^2 .

C. The Optical Cell

The optical cell was made from two circular Pyrex optical flats, approximately three cm in diameter, fused together around the edges. The distance between the flats was uniform at 0.89 mm (± 0.04 mm) except at the edges. The cell could be raised or lowered vertically 1.5 cm or rotated through an angle of $\pm 15^\circ$.

D. Method of Measurement

To measure $|n_e - n_o| < 1 \times 10^{-3}$, the experimental procedure was the following:

1. Set the polarizers at an angle of 90° to one another.
2. Rotate the crossed polarizers and observe the angles of minimum and maximum transmitted light intensity for only those crystals in the preferred orientation. (The preferred orientation is the one in which the principal refractive indices are in a plane normal to the incident beam. Such crystals can be easily recognized since extinction occurs at intervals of 90° .)

3. Measure the maximum intensity with the polarizers crossed.
4. Set the polarizers parallel to each other and measure the maximum intensity.

3.2 Method B.

When it was necessary to resort to method B (i.e. when the birefringence exceeded $\sim 1 \times 10^{-3}$), advantage was taken of the existence of a scheme widely used in mineralogy (Bloss, 1961). With an estimate of the thickness of a crystal fragment, and an Interference Colour Chart (Bloss, 1961 p.144), it is only necessary to determine the maximum interference colour at 45° off extinction in order to estimate the birefringence.

The principles involved are the same as in method A. For incident white light, equation 3.1 becomes a summation over all wavelengths. The colour observed depends on the phase difference α . For a constant light source and principal refractive indices, α varies with the thickness of the crystal-lites. The strongest colourations occur at 45° , 135° , 225° and 315° from the angles of minimum intensity.

The optical system in method B is the same as that used in method A but without the filter to alter the incident beam.

The first two steps in the method of measurement are the same as in method A. The next step is to determine the maximum interference colour with the polarizers crossed and to estimate the crystal thickness. Because the solid shattered into fragments of dimensions less than 0.89 mm in the birefringent phases, the crystal thickness was estimated by taking an average of the two measurable dimensions. The dimensions of the crystal fragments were obtained from the

thickness of the cross-hairs on the eyepiece. The thickness of the cross-hairs was found to be .045 mm, and the dimensions of the crystals were estimated to within half the width of a cross-hair. Since the method of estimating the thickness of the crystallites is rather crude, the uncertainty in the birefringence is approximately $\pm 50\%$.

3.3 Thermal Analysis

Apparatus of simple construction was used for survey-type thermal analysis of MCF and DCP. The object was simply to detect the temperatures at which transitions occurred to guide the determination of optical birefringence of the different phases. A sketch of the apparatus, which was made completely of glass, is shown in figure 3.3.

The sample was distilled into the apparatus from a reservoir in which the sample was degassed by alternate freezing, pumping and melting. It was then cooled relatively slowly with a dry ice-acetone slurry down to 190°K or cooled quickly with liquid nitrogen down to 150°K . Ice-water or water at room temperature were used as baths for the heating of the sample.

Changes in temperature with time were recorded with a Rikadenki recorder, model B-107. The temperature was measured with a five-junction copper-constantan thermocouple connected to the recorder. In order to use the maximum sensitivity of the recorder and to keep the indications of the thermocouple on scale, the thermocouple potential was compensated by an adjustable bucking voltage generated with

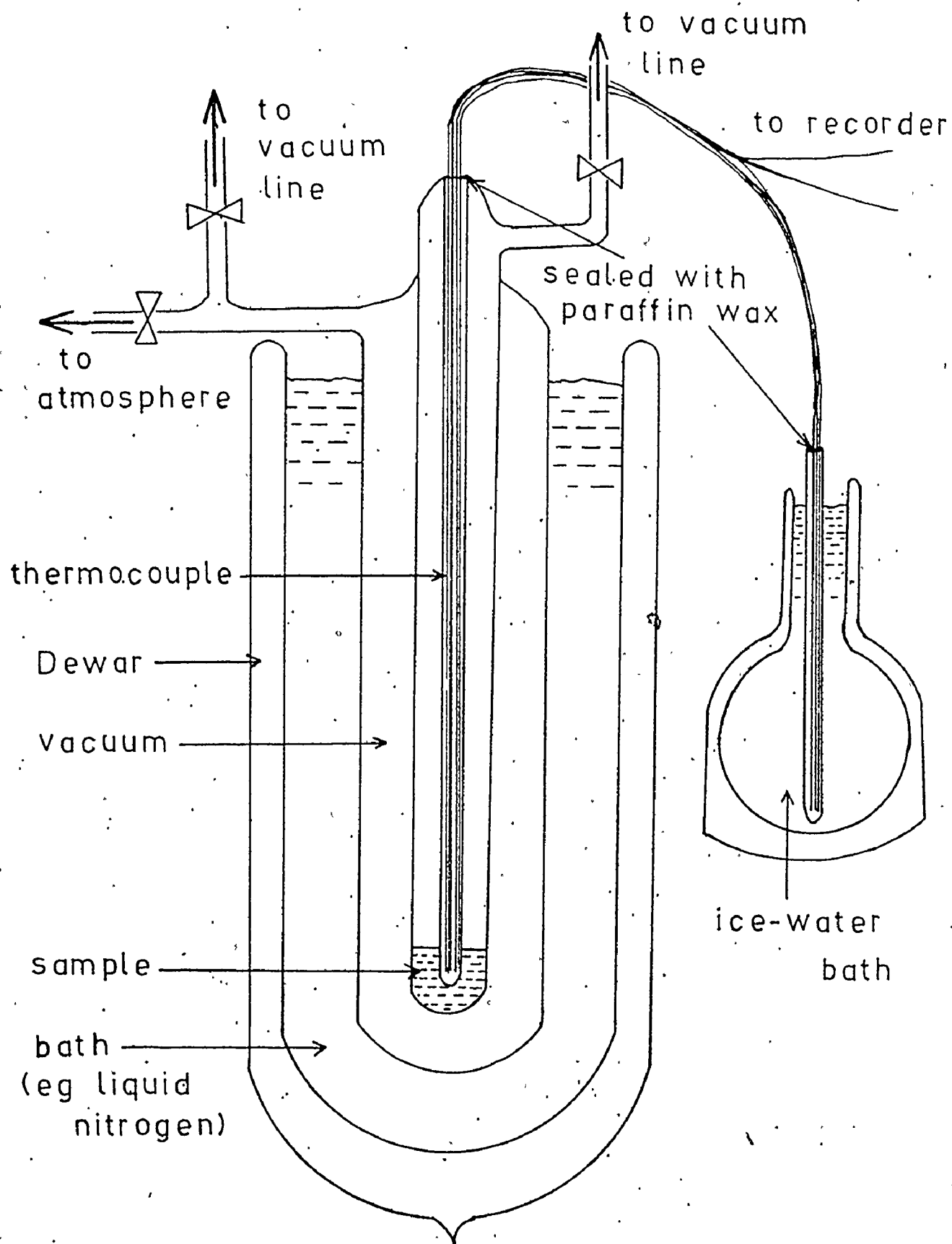


Figure 3.3 Apparatus for thermal analysis

a simple Zener diode circuit. With this apparatus, a temperature difference of 0.2° could be detected. Since an accurate knowledge of absolute values of temperature was not vital, a standard temperature-emf calibration table for a copper-constantan thermocouple was used. The absolute temperatures were probably accurate to within 3° .

3.4 Materials

Research grade MCF was obtained from Chemical Procurement Labs. Inc. and DCP from the J. T. Baker Chemical Co. Further purification of both liquids by preparative vapour phase chromatography with an XF-11-50 fluorinated Carbowax column increased the purity to better than 99.5% for MCF and probably to comparable purity for DCP.

A second sample of MCF was purified with an analytical gas chromatograph using an SE 30 on Chromosorb W column. The purity of this sample, as determined by calorimetry, was 99.2%. The two samples of MCF will be denoted by MCF(I) and MCF(II); respectively.

CHAPTER 4

RESULTS

4.1 Thermal Analysis

Typical time-temperature traces for the thermal analysis of MCF(I) and DCP are shown in figures 4.1a, 4.1b, 4.2a and 4.2b. Apparent supercooling of the different phases always occurred because the temperature usually changed rather rapidly (~ 4 deg/min just before freezing). In order to delineate the transition temperatures in the heating curves more clearly, "effective" Newton's Law constants, k_{eff} , were computed from

$$\frac{dT}{dt} = k_{\text{eff}} (T_{\text{cell}} - T_{\text{bath}}) \quad (4.1)$$

where T is the temperature in $^{\circ}\text{K}$ and t , the time in minutes.

Plots of $|k_{\text{eff}}|$ against T are shown in figures 4.3 and 4.4. In the absence of transitions that absorb energy, $|k_{\text{eff}}|$ would be expected to increase slowly but smoothly with increasing temperature. The transitions are marked by the temperatures where $|k_{\text{eff}}|$ decreases markedly denoting absorption of energy. While, as the error bars show, the uncertainties in the temperatures are fairly large, the semi-quantitative information derived from the thermal analyses was a rather valuable guide for the birefringence experiments.

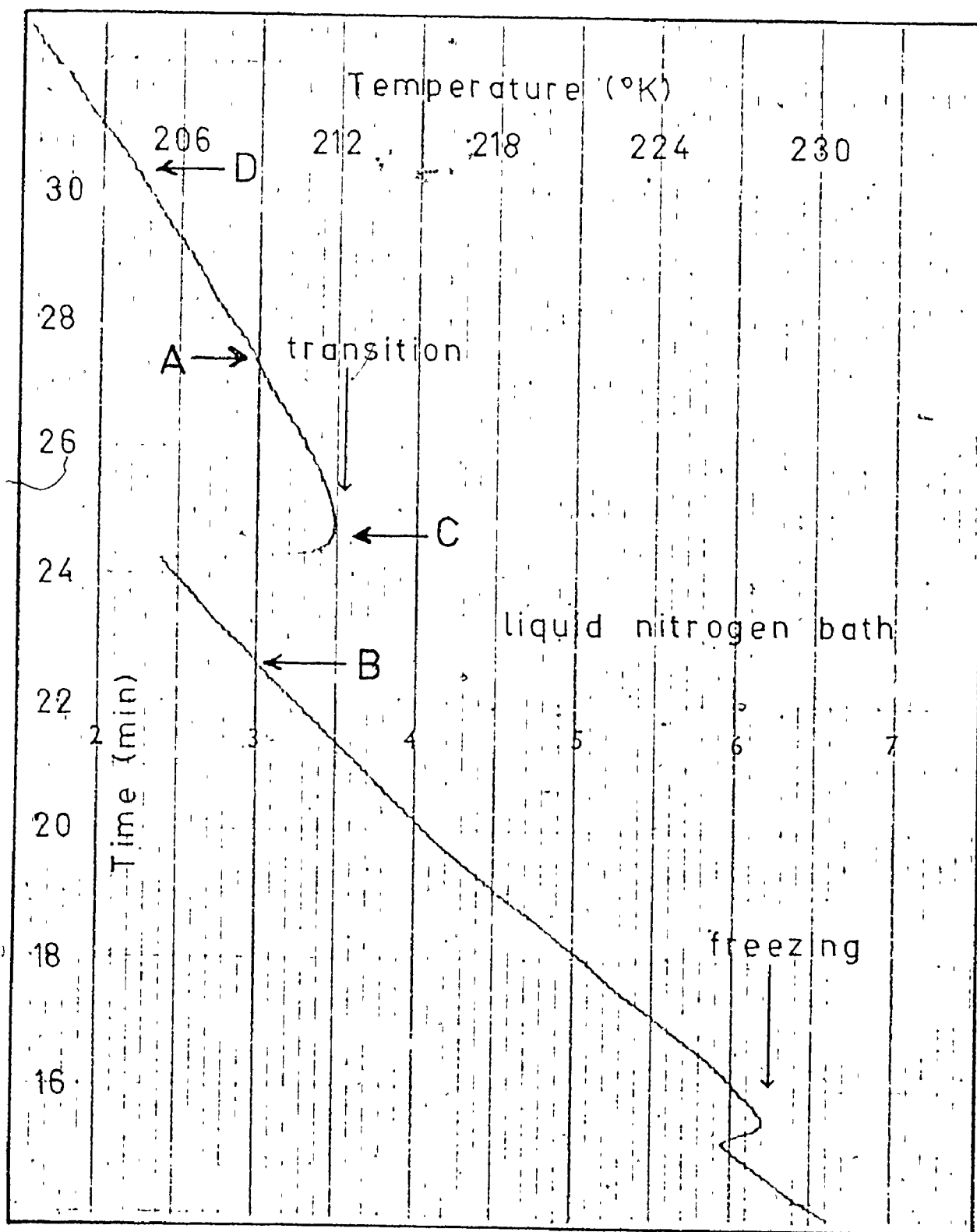


Figure 4.1a Portion of a cooling curve for MCF(I)
(thermal analysis)

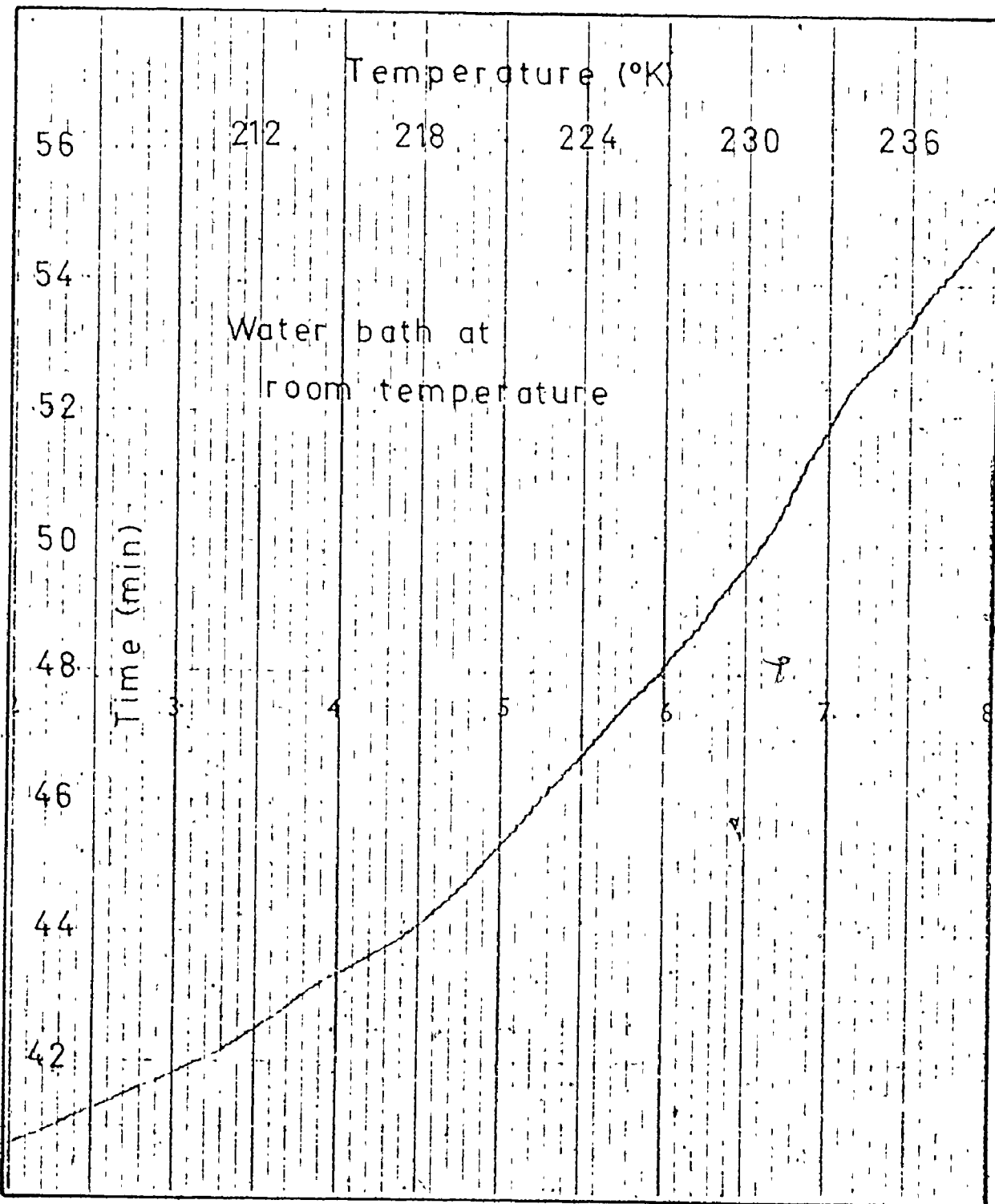


Figure 4.1b Portion of a heating curve for MCF(I) (thermal analysis)

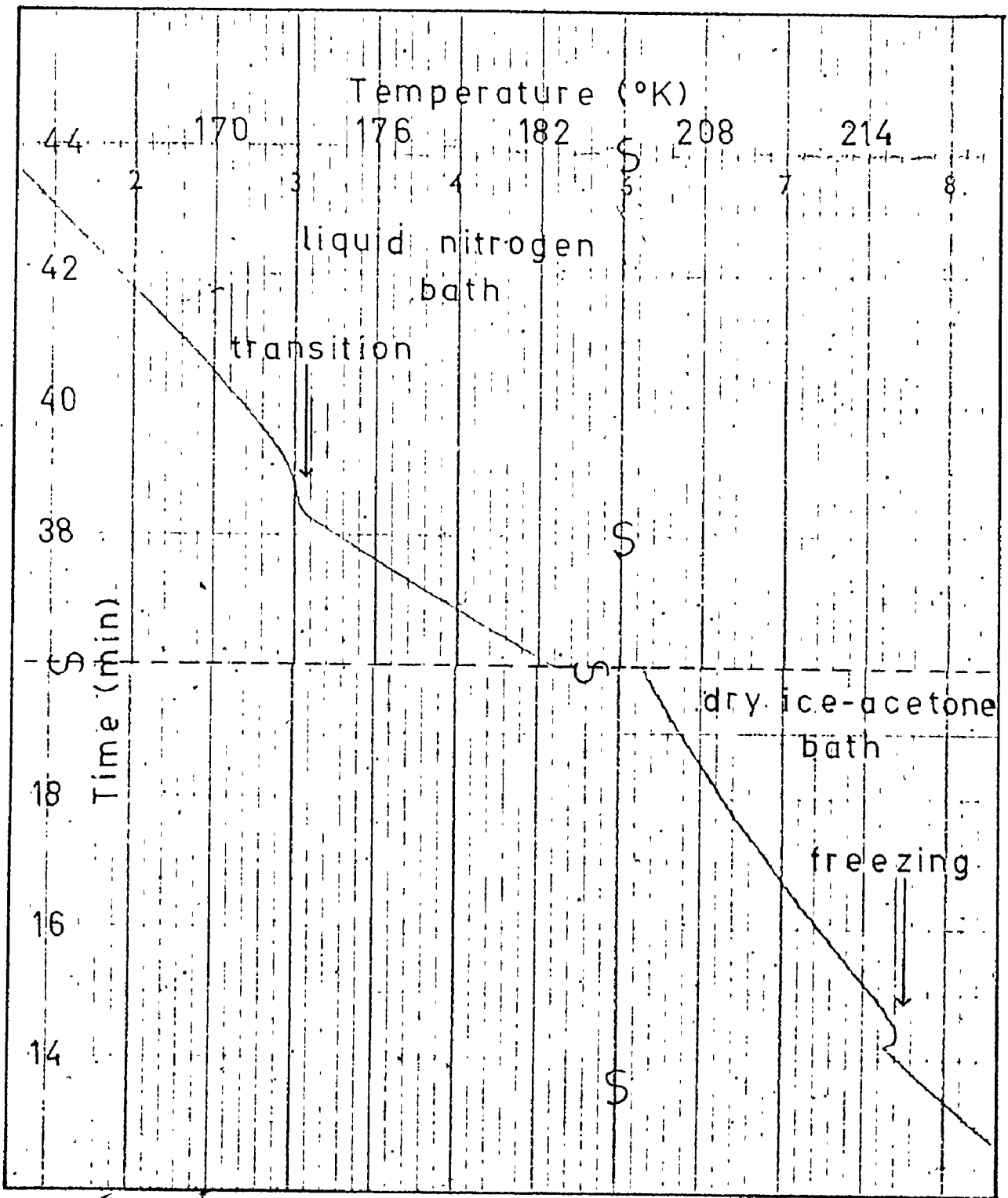


Figure 4.2a Portion of a cooling curve for DCP (thermal analysis)

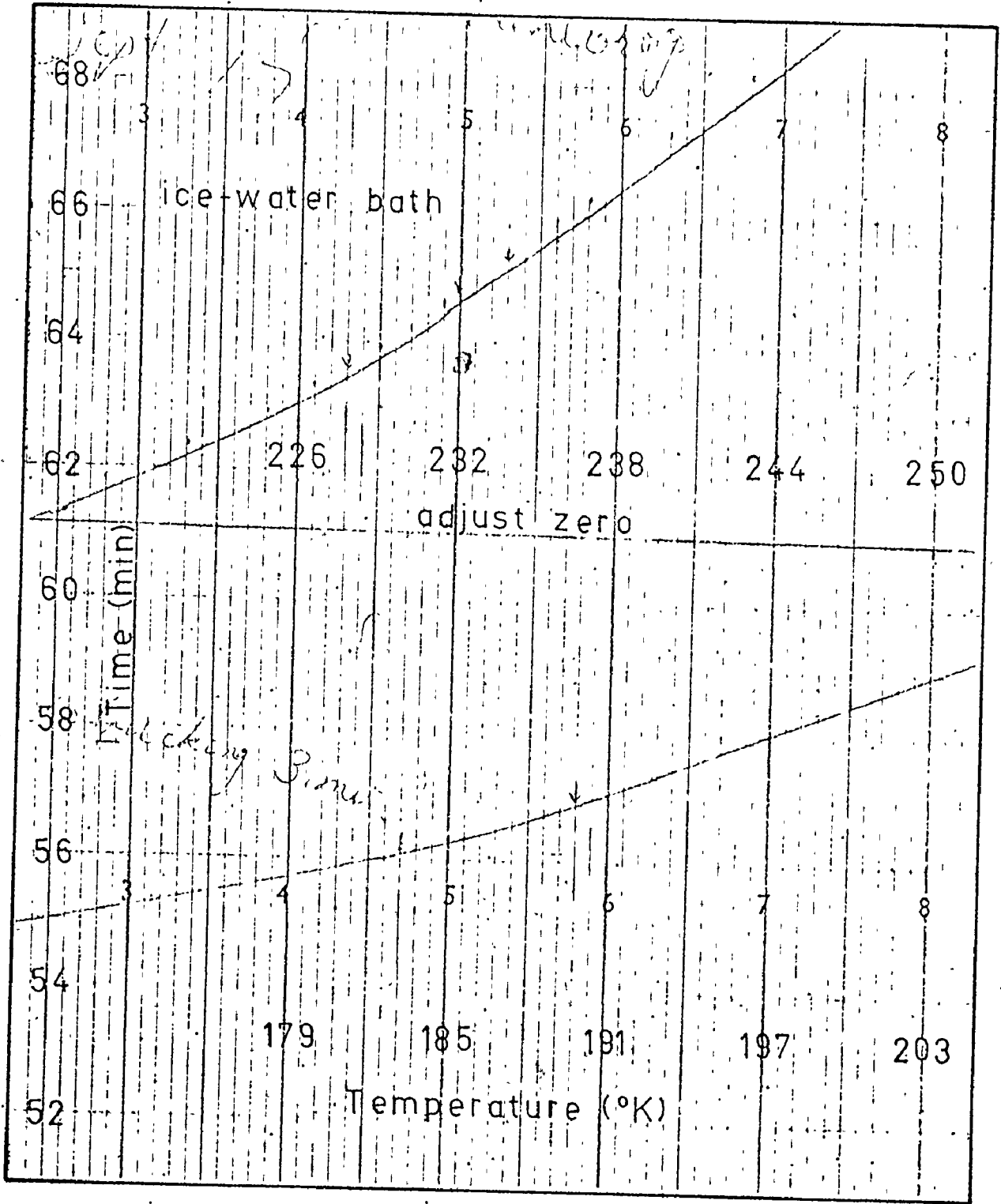


Figure 4.2b Portion of a heating curve for DCP (thermal analysis)

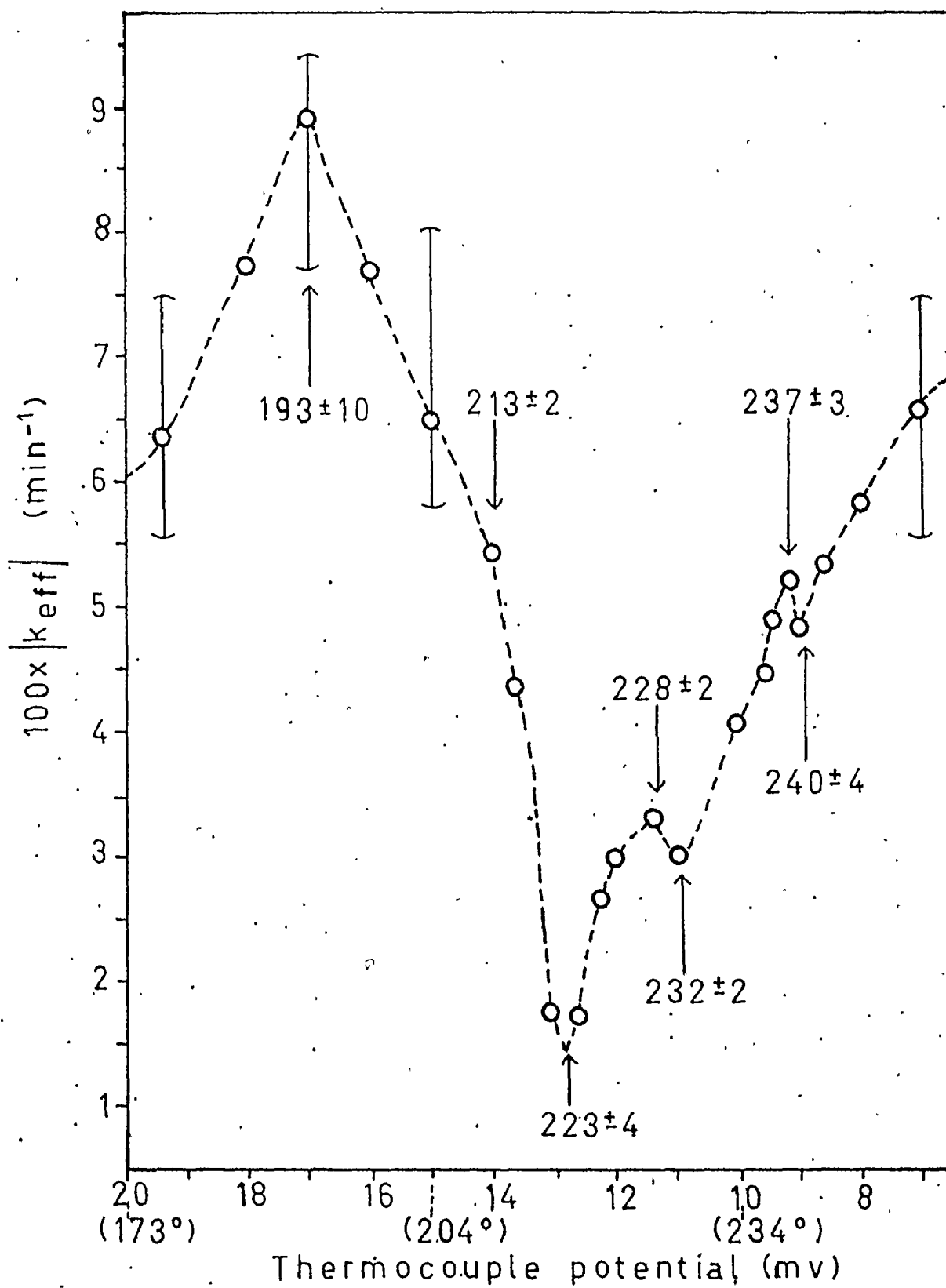


Figure 4.3 Plot of $|k_{\text{eff}}|$ versus temperature for MCF

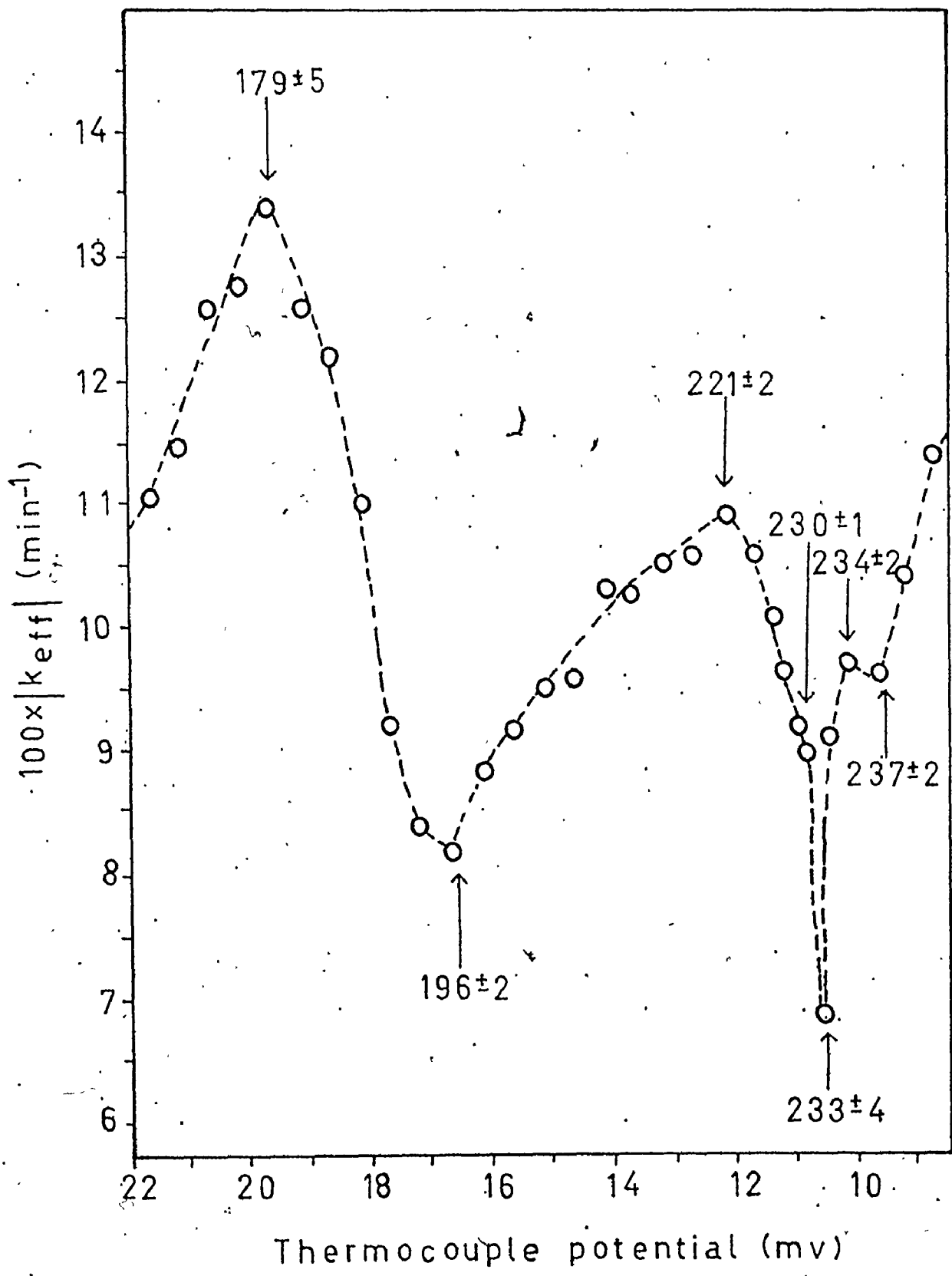


Figure 4.4 Plot of $|k_{eff}|$ versus temperature for DCP

In MCF(I) it was found that, on cooling, energy was released after the large transition peak. This was indicated by the difference in the slopes of the temperature vs time plot at a given temperature.

In figure 4.1a the slope at point A was found to be significantly less than that at point B. This release of energy from point C to point D corresponded to the energy absorbed on heating in the $193^{\circ} < T < 213^{\circ} \text{K}$ range. It was thought at first that this behavior might be an indication of a transition to a phase III of MCF, something about which there have been conflicting findings (Rubin et al, 1944; Crowe and Smyth, 1950; Silver and Rudman, 1972). However, this "extra" release and absorption of energy was not observed in later calorimetric measurements (Morrison et al, 1976) so that the effect in the thermal analysis probably arises from considerable thermal inertia displayed by the I to II transition:

Table 4.1 summarizes the results obtained from the thermal analyses. The correlations of phase changes in MCF(I) and DCP suggested by these results are depicted in figures 4.5 and 4.6.

4.2 Birefringence

The birefringence studies established the existence of three solid phases in both MCF and DCP. Both compounds have a non-birefringent phase, which will be called phase Ia following the nomenclature used by Rudman and Post (1968), a moderately birefringent phase called phase Ib and a highly birefringent phase labelled phase II.

TABLE 4.1 Temperatures of Phase Changes from the Thermal Analyses of MCF and DCP

| MCF | Temperature of Phase Changes |
|--------------------------------------|----------------------------------|
| Freezing, melting | 227(±3), 228(±2) - 240(±4) |
| Transition (cooling), (heating) | 212(±1), 213(±2) - 223(±4) |
| After transition, pre- transition | 212 - 188, 193(±10) |
| DCP | Temperature of Phase Changes |
| Freezing, melting | 219(±3), 230(±1) - 237(±2) |
| Transition (heating) | 221(±2) - 230(±1) |
| Transition (cooling), (heating) | 174(±3) - 167, 179(±5) - 196(±2) |

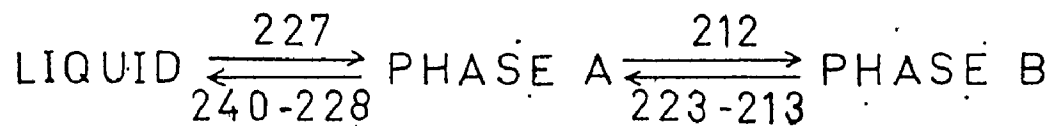


Figure 4.5 Phase changes in MCF(I) deduced from thermal analysis

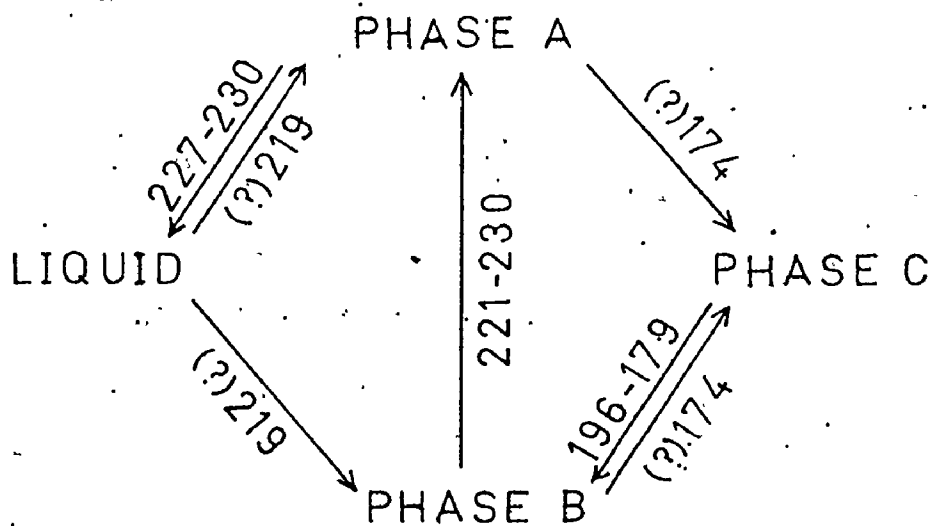


Figure 4.6 Phase changes in DCP deduced from thermal analysis

In MCF(I), which was 99.5% pure, only phase Ia and phase II were observed. In MCF(II), which was 99.2% pure, a reproducible and moderately birefringent phase (phase Ib) formed on cooling phase Ia. Phase Ib melted without transforming into phase Ia first.

The measured birefringences are summarized in table 4.2. The level of $|n_e - n_o|$ in phase Ia of both MCF and DCP is accountable for by strain. Indeed, in MCF(I), the initial values were of the magnitude of 4×10^{-5} which slowly decreased to $< 1 \times 10^{-5}$ as the phase Ia annealed.

The estimate of $|n_e - n_o|$ for phases II is a lower limit. When they formed, the crystallites were so small that it was difficult to estimate their dimensions. Moreover, they scattered most of the incident light and colour changes could only be recognized with great difficulty.

Since the phase changes could be observed through the eyepiece, and the changes correlated with the temperature of the cell, the variation from run to run with the rate of heating and cooling could be observed. The amount of variation is indicated by the uncertainties given for the transition temperatures in table 4.3.

Because of supercooling, fairly sharp freezing and transition temperatures were observed for cooling, while, for heating, the transitions and melting occurred over a temperature range or over a period of hours. In table 4.3 the temperatures listed correspond to the temperatures at which the solids were completely melted or transformed. Rapid

TABLE 4.2 Birefringence of the Solid Phases of MCF and DCP

| | MCF | DCP |
|----------|---------------------|---------------------|
| Phase Ia | $<1 \times 10^{-5}$ | $<1 \times 10^{-5}$ |
| Phase Ib | .003(\pm .001) | .011(\pm .006) |
| Phase II | $>10^{-2}$ | $>10^{-2}$ |

TABLE 4.3 Temperatures of Phase Changes from the Birefringence Study of MCF and DCP

| MCF | Temperature of Phases Changes |
|--|-------------------------------|
| Liquid \rightarrow Ia, Ia \rightarrow liquid | 229(\pm 4), 253(\pm 6) |
| Liquid \rightarrow Ib, Ib \rightarrow liquid | * , 249 |
| Ia \rightarrow Ib, Ib \rightarrow Ia | 214 , * |
| Ia \rightarrow II, II \rightarrow Ia | 208(\pm 8), 231(\pm 3) |
| Ib \rightarrow II, II \rightarrow Ib | 198 , \sim 230 |
| DCP | Temperature of Phase Changes |
| Liquid \rightarrow Ia, Ia \rightarrow liquid | 248 , 243(\pm 5) |
| Liquid \rightarrow Ib, Ib \rightarrow liquid | 221(\pm 7), 253 |
| Ia \rightarrow Ib, Ib \rightarrow Ia | * , 206 ** |
| Ib \rightarrow II, II \rightarrow Ib | 169(\pm 7), 201(\pm 9) |

NOTE: Temperatures given with no variation were single observations.

*Transition not observed

**At 206°, Ib transformed into Ia after one day.

heating may have caused superheating or the transitions may have been affected by hysteresis. Figure 4.7a,b,c,d is a section of a temperature-time plot for DCP and illustrates how the various phases can change or persist as the temperature is varied over a long period of time. Similar plots can be drawn for results for MCF(I) and MCF(II).

The sequence of phase transitions is represented schematically in figure 4.8. The large differences in the temperatures given for cooling and heating are undoubtedly due to the non-equilibrium conditions pertaining. Thus, the temperatures for the transitions obtained in the birefringence studies are rather rough compared to what can be obtained with careful calorimetric measurements.

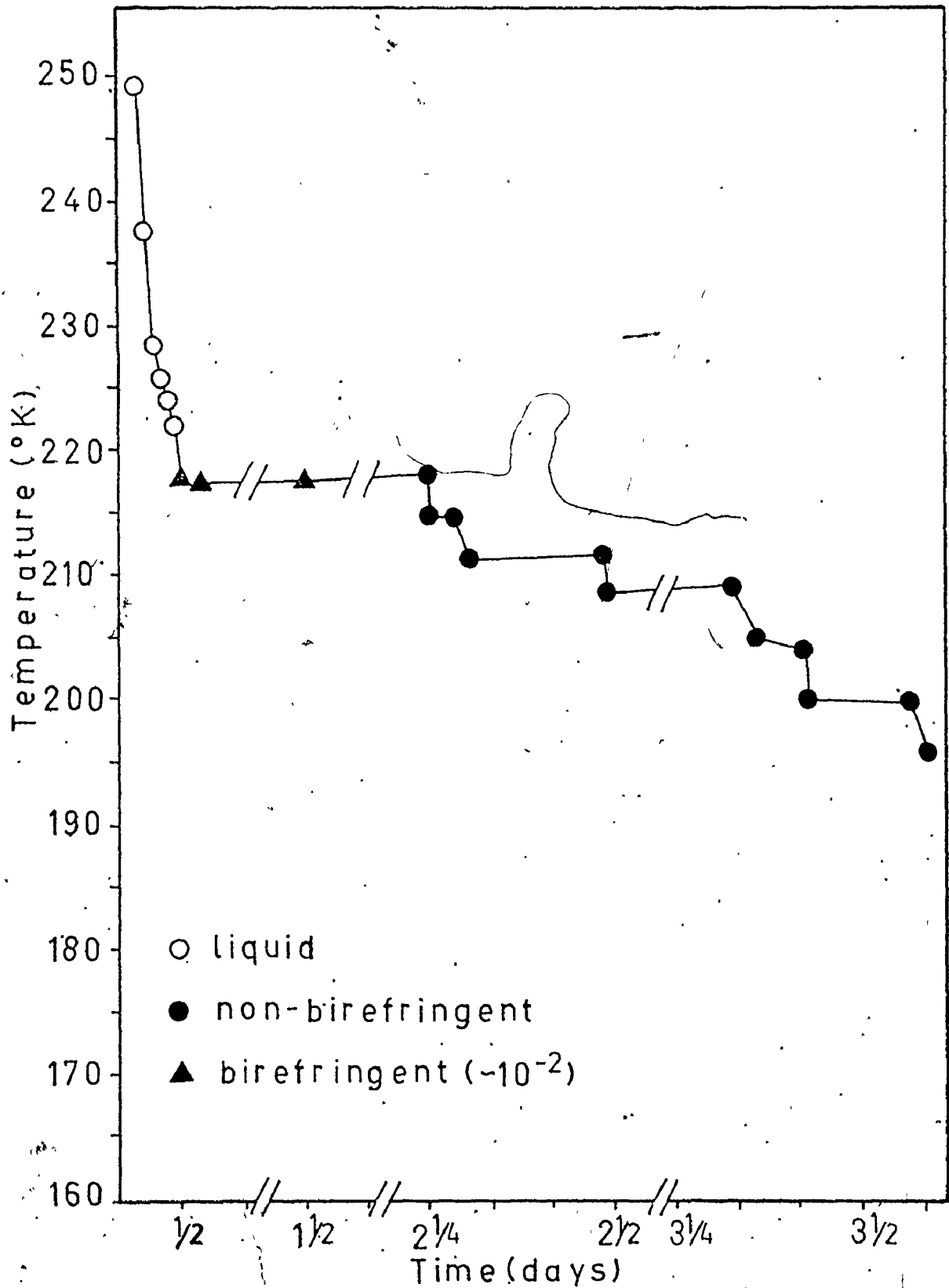


Figure 4.7a Plot of temperature versus time for DCP (birefringence measurements)

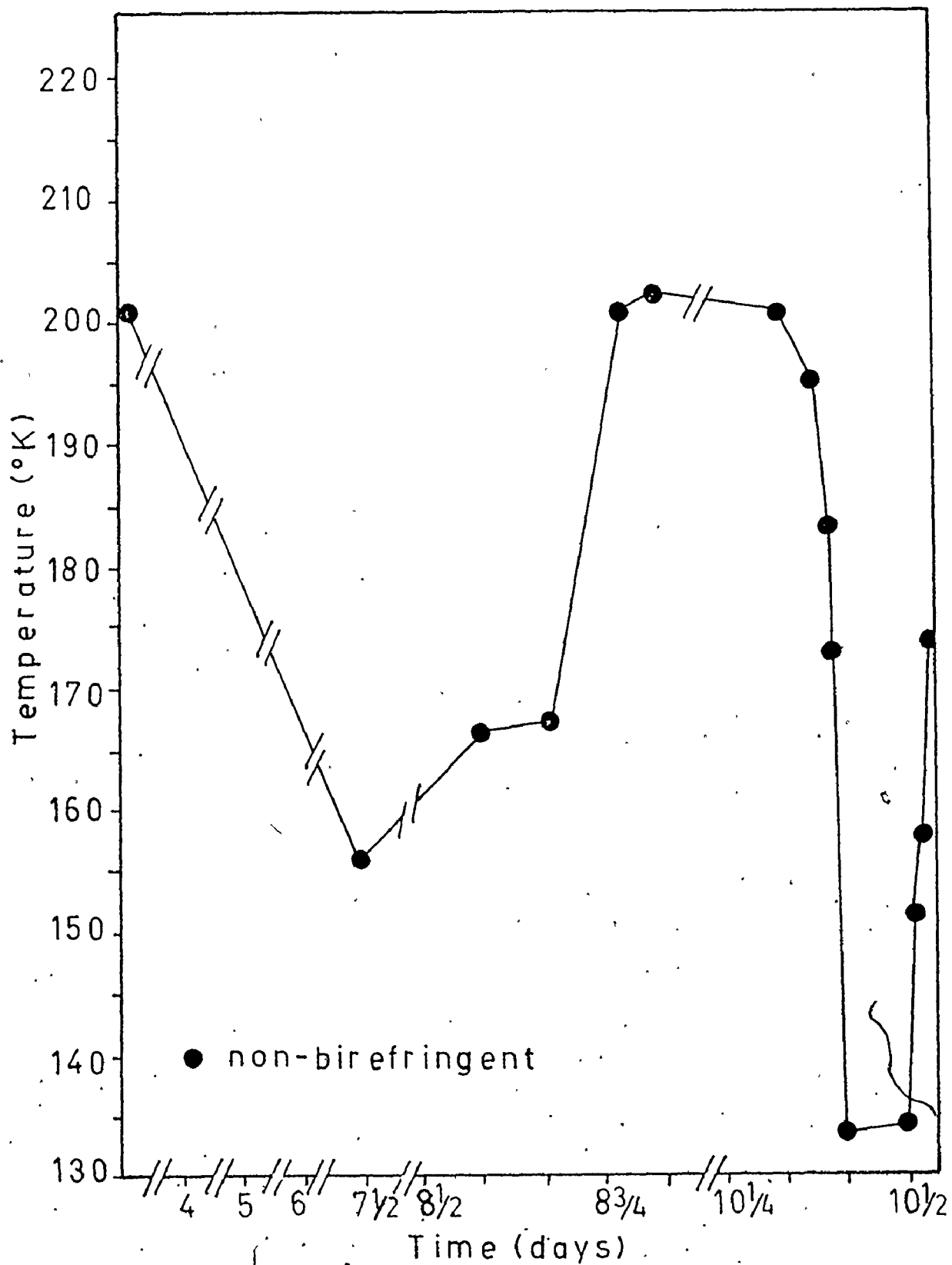
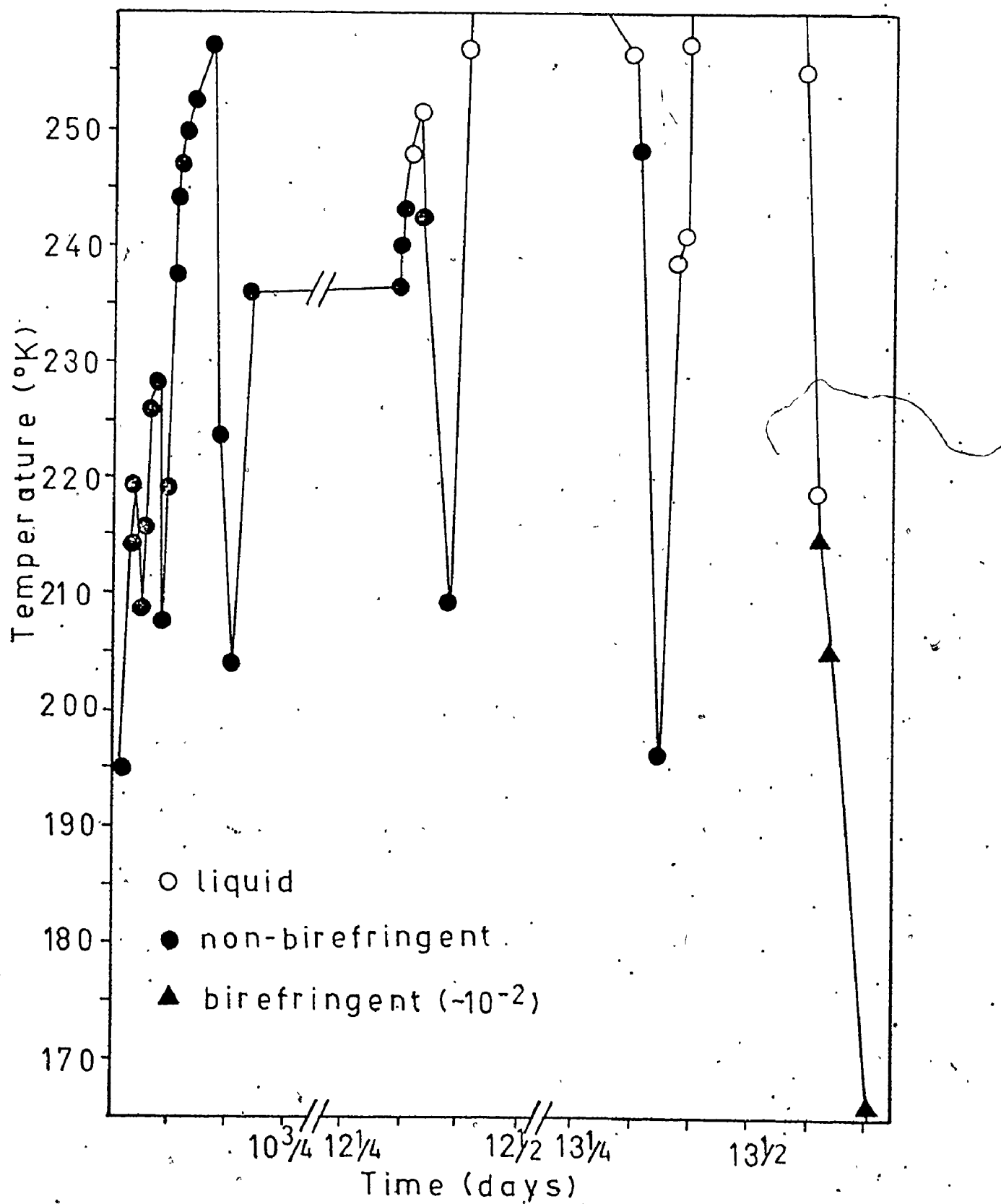


Figure 4.7b Plot of temperature versus time for DCP (birefringence measurements)



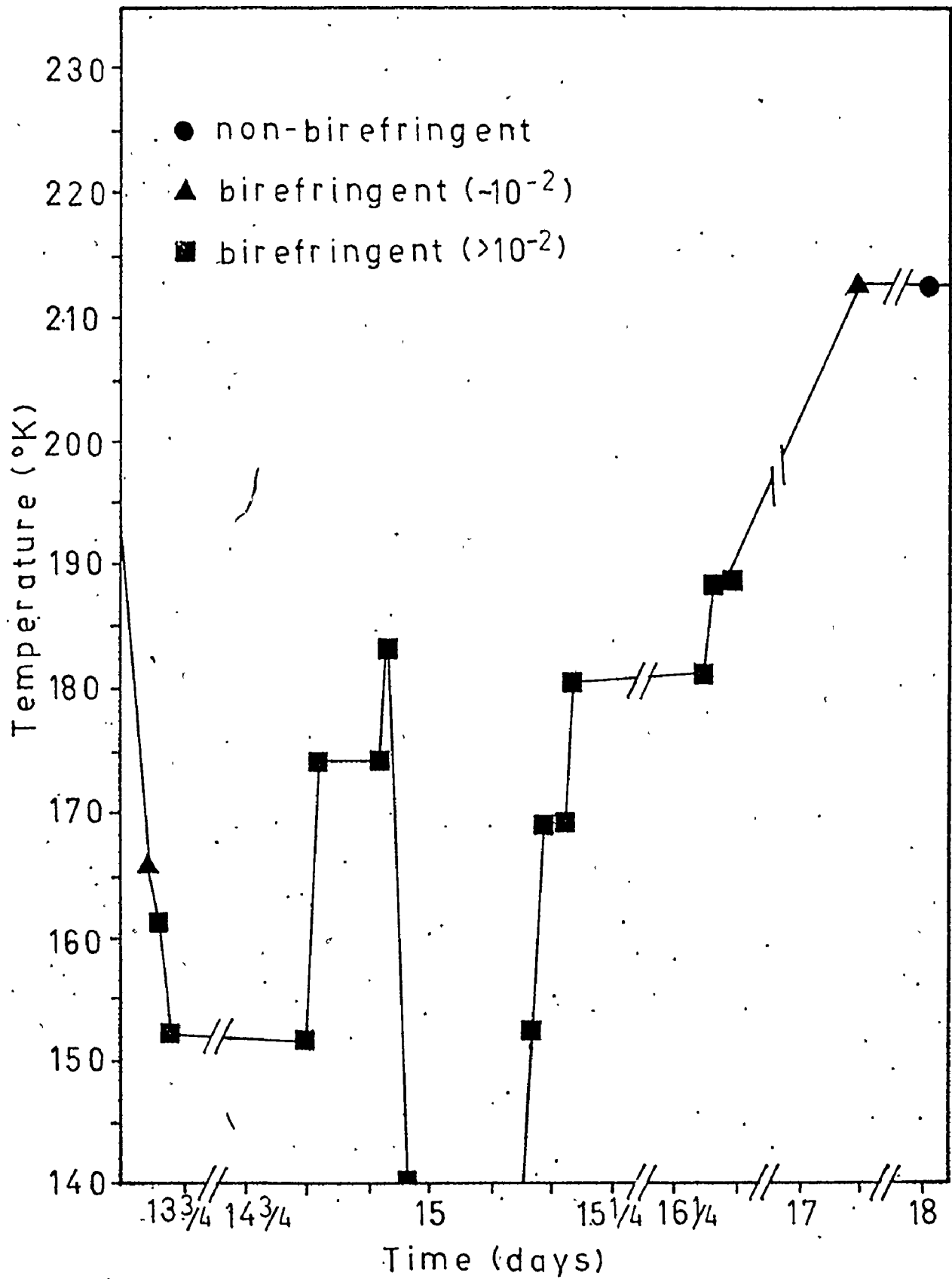
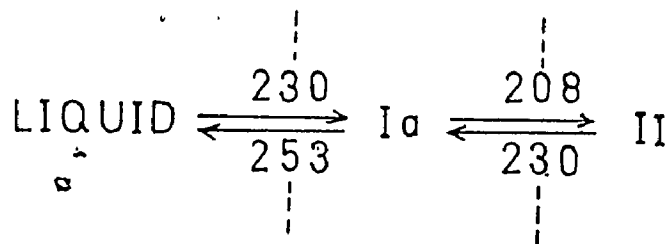
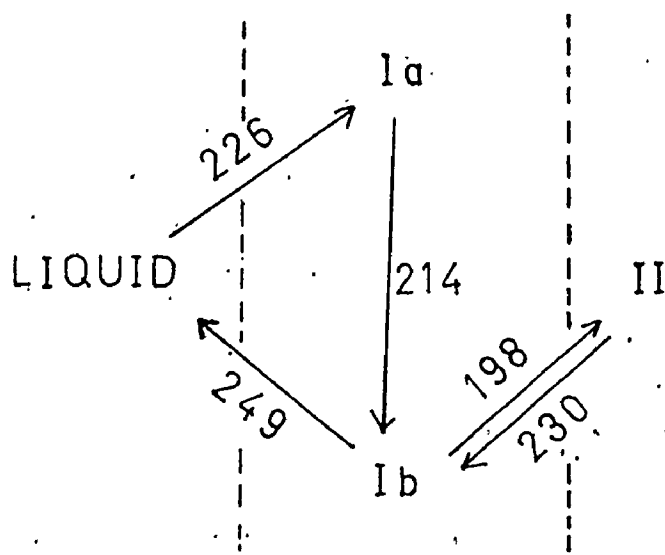


Figure 4.7d Plot of temperature versus time for DCP (birefringence measurements)

MCF (I)



MCF (II)



DCP

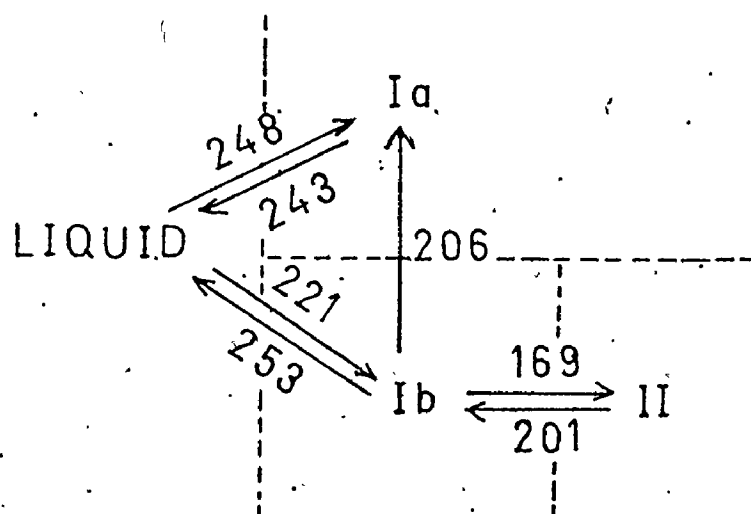


Figure 4.8 Phase transitions in MCF and DCP deduced from birefringence studies

CHAPTER 5

DISCUSSION

The phenomenological understanding of polymorphism in MCF and DCP before this birefringence study was undertaken was the following:

(i) MCF and DCP formed a face-centred cubic phase Ia and an orthorhombic phase II. Similar to CCl_4 , both solids formed a second plastic phase labelled phase Ib. However, in MCF, phase Ib was reported to be cubic while, in DCP and CCl_4 , it was rhombohedral.

(ii) Little was known about the sequence of transitions in DCP. In fact, Silver and Rudman (1970) described phase Ia and phase Ib as occurring "nearly simultaneously".

(iii) The difference in transition temperatures on heating and cooling were great due to the effects of supercooling and hysteresis.

(iv) Some researchers (e.g. Silver and Rudman, 1972) had questioned the existence of a phase III in MCF.

The present study has added the following information:

(i) There are two plastic phases in MCF and DCP but only one is cubic. The other has a birefringence comparable to that of phase Ib in CCl_4 for which the structure has been determined to be rhombohedral.

- (ii) No evidence was found for the existence of phase III.
- (iii) The stabilities of the plastic phases appear to be determined by impurities. For example, it was found that MCF(I) only formed phase Ia while the less pure MCF(II) formed phase Ib as well as Ia.

The birefringence study of MCF led to a calorimetric investigation of MCF(I) and MCF(II) in which it was established that the thermal properties of the phases I were measurably different. In particular, the melting points, enthalpies of transition and fusion were different and this general result is consistent with the birefringence deductions.

The additional information obtained from the calorimetric results (Morrison, Richards and Sakon, 1976) giving accurate enthalpies and more precise transition temperatures is summarized in table 5.1.

In general, there are some basic similarities in the polymorphs and the phase transitions in solid CCl_4 , MCF and DCP. They all form two plastic crystal phases and one low temperature solid phase. Structural studies (X-ray and birefringence) show that one phase I is cubic in the three compounds and the other, rhombohedral in CCl_4 and DCP (and possibly in MCF). Melting and freezing of both plastic phases in all three compounds have been observed (for CCl_4 , Morrison and Richards, 1976 and Arentsen and van Miltenburg, 1972; for MCF, Morrison et al, 1976; and for DCP, this research). Only in MCF has the Ia to II transition and its reverse been observed. The formation of phase II is well-defined and consistent while the formation of phase Ia and phase Ib

TABLE 5.1 Summary of Calorimetric Measurements on MCF

| Transitions in MCF(I) | Temperatures of transition ($^{\circ}\text{K}$) | ΔH (J/mole) |
|---------------------------|--|---------------------------|
| Liquid \rightarrow Ia | 234 | |
| Ia \rightarrow II | | |
| II \rightarrow Ia | 224.3 ± 0.1 | 7450 ± 75 |
| Ia \rightarrow Liquid | 243.0 ± 0.3 | 2380 ± 45 |
| Transitions in MCF(II) | Temperatures of transition ($^{\circ}\text{K}$) | ΔH (J/mole) |
| Liquid \rightarrow Ib | 229 | |
| Ib \rightarrow II | | |
| II \rightarrow Ib | 223.9 ± 0.1 | 7715 ± 100 |
| Ib \rightarrow Liquid | 240.9 ± 0.3 | 2125 ± 50 |

on experimental conditions.

The summary by Rudman and Post (1968) can now be altered to show that high purity MCF exhibits only two solid polymorphs, phase Ia and II. Lower purity MCF exhibits an additional phase I which is intermediate in birefringence between that of phase Ib in CCl_4 and of phase Ib in DCP. Analysis of calorimetric data for melting shows the impurity to be essentially insoluble in solid MCF (Morrison et al, 1976). This suggests that perhaps the impurities act as nucleation sites for the crystallization of phase Ib.

In DCP, phase Ia was found to be more stable than phase Ib. Phase Ib transformed into phase Ia at high temperatures and, once formed, phase Ia never transformed into phase Ib or II even at very low temperatures (120°K). However, it is possible that phase Ia may be stabilized by the glass optical cell. In their birefringence studies of CCl_4 , Koga and Morrison (1975) found that the phase Ib to Ia transition did occur and that phase Ia persisted for several days. Also van Miltenburg (1971) found that the phase Ia to Ib transition did not occur for CCl_4 in a full glass container and he has suggested that the material from which the sample container is made, influences the transition. This is supported by the finding that phase Ib was more stable than Ia (in fact, the phase Ib to Ia transition did not occur) in calorimetric measurements of CCl_4 using sample containers made from metal (Arentsen and van Miltenburg, 1972 and Morrison and Richards, 1976).

In the DCP, it has been shown that the liquid can freeze into phase Ia or phase Ib but not "nearly simultaneously". Phase Ib can transform into Ia or II but the Ia \rightleftharpoons II transformations never occur. A calorimetric study by van Miltenburg (1972) revealed only two solid phases. This is not in disagreement with the present study since it has been shown that the II \rightarrow Ib \rightarrow liquid sequence does occur and that the phase Ib to Ia transformation is slow. It is likely that, in order to obtain phase Ia, the solid will have to be heated slowly or heated before reaching the Ib to II transition temperature. Once phase Ia is obtained, it may be reproduced if freezing of the DCP is done immediately after melting. The formation of phase Ia will probably be enhanced with the use of a sample container made of glass.

In sum, the combination of X-ray, birefringence and calorimetric studies can reveal much about the polymorphs and their transitions in the solid methylchloromethane compounds.

CHAPTER 6

CONCLUSIONS

The results described in this thesis together with data derived from some other kinds of experiments show that two different solid phases of MCF can exist in the same temperature range. One is cubic and the other non-cubic. They are labelled phases Ia and Ib, in the terminology adopted by Rudman and Post (1968). However, the deductions made here about them differ significantly from proposals made by Rudman and Post. In the first place, it is now clear that the existence of the phases depends critically on the purities of the MCF specimens. Thus, we have been able to obtain either Ia or Ib and to transform them reversibly into the lower symmetry phase II. This behavior contrasts with that of CCl_4 where phase Ia is metastable with respect to phase Ib. In the second place, phase Ib is markedly birefringent and so its structure is clearly non-cubic. Rudman and Post (1968) proposed that this phase was primitive cubic and that its formation required special thermal treatment of the specimen tube. It is always possible that the phase Ib observed in this research may be different from the one observed by Rudman and Post but this is doubtful.

Because there is much less information available about the thermal properties of DCP, less firm deductions can be made about polymorphism in that substance. However, the birefringence study shows unambiguously that three solid phases exist - one cubic and two non-cubic.

It is possible that birefringence measurements on t-butyl chloride and neopentane would yield a second plastic phase in these compounds which has not been observed. Since very weak birefringences are difficult to detect with the X-ray diffraction apparatus, a phase Ib may have been overlooked. Further calorimetry on the MCM compounds $(\text{CH}_3)_n \text{CCl}_{(4-n)}$ for $n = 2, 3$ and 4 would give accurate transition temperatures and additional thermal data. This has been done recently for MCF (Morrison et al (1976)) and has proven to be invaluable in the understanding of the polymorphic transitions in solid MCF.

The structural data which are in doubt should now be rechecked with X-ray measurements. This is especially important for MCF since the present research indicates that phase Ib probably was not obtained by Rudman and Post (1968) in their structural studies.

The need for a study of the factors influencing the relative stabilities of the different phases of these compounds is also indicated. Thus, further research is required before a more comprehensive comparison of the MCM compounds can be made.

REFERENCES

- Arentsen, J.G., Miltenburg, J.C. van, 1972, *J. Chem. Thermodynamics*, 4, 789.
- Ballik, E.A., Gannon, D.J., and Morrison, J. A., 1973, *J. Chem. Phys.* 12, 5639.
- Bloss, F.D., 1961, An Introduction to the Methods of Optical Crystallography (Holt, Rinehart and Winston, New York) Chaps. 6-8.
- Born, M. and Huang, K., 1954, Dynamical Theory of Crystal Lattices (Oxford University Press, London) Chap.5..
- Chihara, H. and Koga, Y., 1971, *Bull. Chem. Soc. Jap.* 44, 2681.
- Cowley, E. R., 1970, *Can. J. Phys.* 48, 297.
- Crowe, R.W. and Smyth, C.P., 1950, *J. Amer. Chem. Soc.* 72, 4009.
- Hicks, J.F.G., Hooley, J.G. and Stephenson, C.C., 1944, *J. Amer. Chem. Soc.* 66, 1064.
- Koga, Y. and Morrison, J.A., 1975, *J. Chem. Phys.* 62, 3359.
- Miltenburg, J.C. van, 1971. Construction of an Adiabatic Calorimeter and Measurement of the System Carbon Tetrachloride + Cyclohexanone, Doctoral thesis (Rijksuniversiteit Utrecht).
- Miltenburg, J.C. van, 1972, *J. Chem. Thermodynamics*, 4, 773.
- Morrison, J.A. and Richards, E.L., 1976, *J. Chem. Thermodynamics* - in press.

Morrison, J.A., Richards, E.L. and Sakon, M., 1976 - to be published.

Post, B., 1959, Acta Cryst. 12, 349.

Rubin, T.R., Levedahl, B.H. and Yost, D.M., 1944, J. Amer. Chem. Soc. 66, 279.

Rudman, R., 1970, Mol. Cryst. Liquid Cryst. 6, 427.

Rudman, R. and Post, B., 1966, Science 154, 1009.

Rudman, R. and Post, B., 1968, Mol. Cryst. 5, 95.

Silver, L. and Rudman, R., 1970, J. Phys. Chem. 74, 3134.

Silver, L. and Rudman, R., 1972, J. Chem. Phys. 57, 210.

Timmermans, J., 1961, J. Phys. Chem. Solids 18, 1.